AD-A119 390 COLD REGIONS RESEARCH AND ENGINEERING LAB HANOVER NH F/G 8/11
SEISMIC SITE CHARACTERIZATION TECHNIQUES APPLIED TO THE NATO RS--ETC(U)
JUL 82 D G ALBERT
UNCLASSIFIED CRREL-82-17 NL

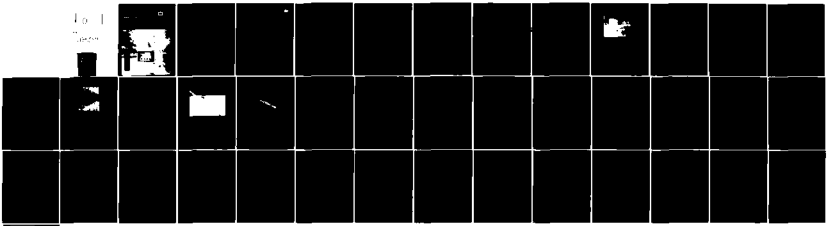

END
DATE
FILMED
10 82
DTIC

(12)

CRREL REPORT 82-17

US Army Corps of Engineers
Cold Regions Research & Engineering Laboratory

Seismic site characterization techniques applied to the NATO RSG-11 test site in Münster Nord, Federal Republic of Germany

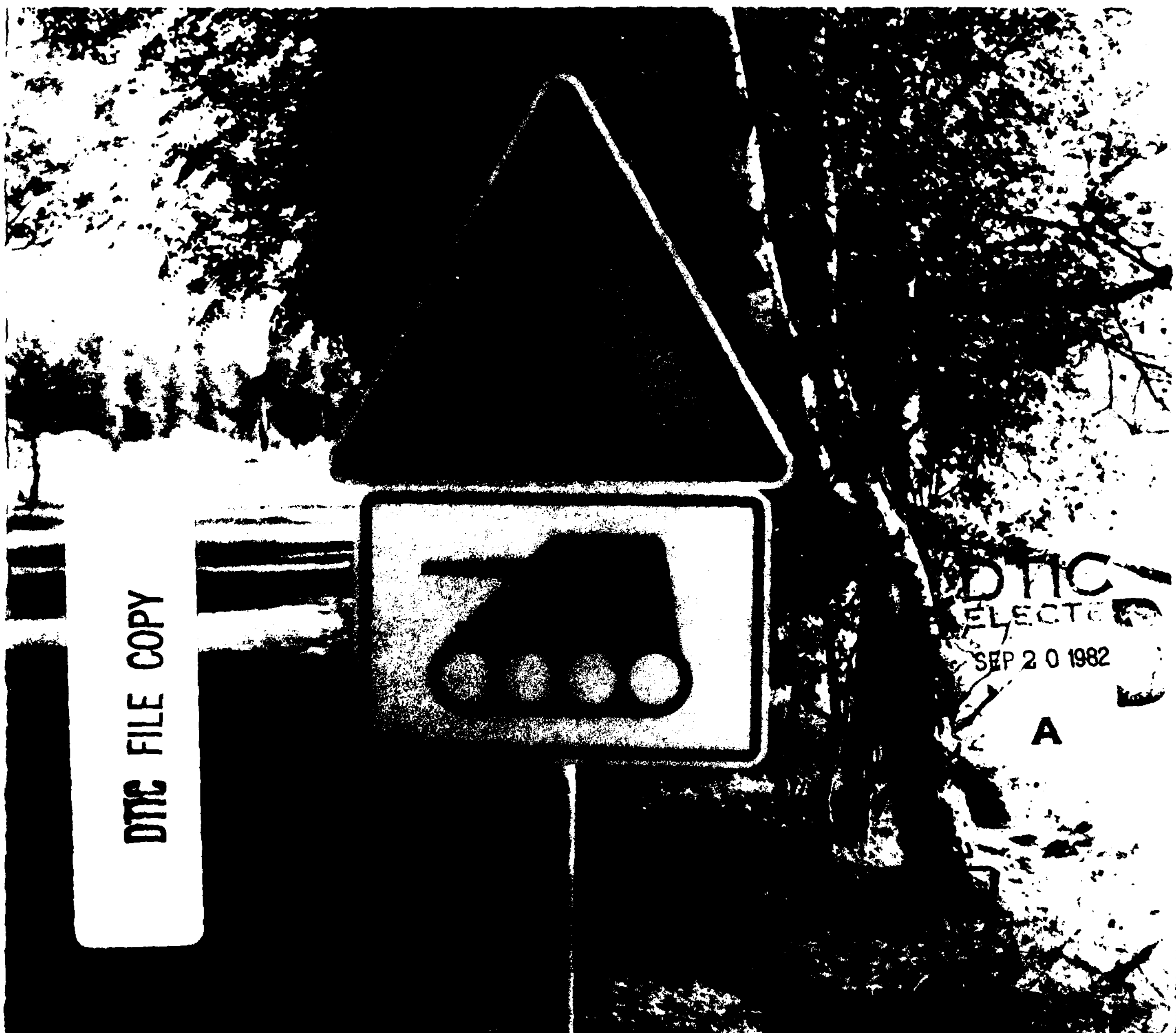

For conversion of SI metric units to U.S./ British customary units of measurement consult ASTM Standard E380, Metric Practice Guide, *published by the American Society for Testing and Materials, 1916 Race St., Philadelphia, Pa. 19103.*

Cover: *Warning sign near the NATO vehicle test site at Münster Nord, Federal Republic of Germany.*

CRREL Report 82-17

July 1982

Seismic site characterization techniques applied to the NATO RSG-11 test site in Münster Nord, Federal Republic of Germany

Donald G. Albert

Prepared for
OFFICE OF THE CHIEF OF ENGINEERS

Unclassified

SECURITY CLASSIFICATION OF THIS PAGE (When Data Entered)

REPORT DOCUMENTATION PAGE

READ INSTRUCTIONS BEFORE COMPLETING FORM

1. REPORT NUMBER

CRREL Report 82-17

2. GOVT ACCESSION NO.

AD-A119390

3. RECIPIENT'S CATALOG NUMBER

4. TITLE (and Subtitle)

SEISMIC SITE CHARACTERIZATION TECHNIQUES APPLIED TO THE NATO RSG-11 TEST SITE IN MÜNSTER NORD, FEDERAL REPUBLIC OF GERMANY

5. TYPE OF REPORT & PERIOD COVERED

6. PERFORMING ORG. REPORT NUMBER

7. AUTHOR(s)

Donald G. Albert

8. CONTRACT OR GRANT NUMBER(s)

9. PERFORMING ORGANIZATION NAME AND ADDRESS

U.S. Army Cold Regions Research and Engineering Laboratory
Hanover, New Hampshire 03755

10. PROGRAM ELEMENT, PROJECT, TASK AREA & WORK UNIT NUMBERS

DA Project 4A762730AT42
Technical Area B, Work Unit 002

11. CONTROLLING OFFICE NAME AND ADDRESS

Office of the Chief of Engineers
Washington, D.C. 20314

12. REPORT DATE

July 1982

13. NUMBER OF PAGES

37

14. MONITORING AGENCY NAME & ADDRESS(if different from Controlling Office)

15. SECURITY CLASS. (of this report)

Unclassified

15a. DECLASSIFICATION/DOWNGRADING SCHEDULE

16. DISTRIBUTION STATEMENT (of this Report)

Approved for public release; distribution unlimited.

17. DISTRIBUTION STATEMENT (of the abstract entered in Block 20, if different from Report)

18. SUPPLEMENTARY NOTES

19. KEY WORDS (Continue on reverse side if necessary and identify by block number)

Geologic models
NATO
Seismic refraction
Seismic signatures
Seismic surface waves
Seismology
West Germany

20. ABSTRACT (Continue on reverse side if necessary and identify by block number)

Seismic P and SH wave refraction experiments at the NATO RSG-11 test site in Münster Nord, Federal Republic of Germany, reveal the presence of a nearly horizontal, three-layer velocity structure. The upper layer, composed of unconsolidated glacial till, is 1 m thick and has P (compressional) and SH (shear-horizontal) wave velocities of 240 and 165 m/s. The second layer, made up of similar, more compacted material, is 9.5 m thick, with a P wave velocity of 470 m/s and an SH wave velocity of 275 m/s. The third layer, interpreted as the groundwater table, is located at a depth of 10.5 m and has a P wave velocity of 1590 m/s. The SH wave velocity of this layer is controlled by the matrix material and is the same as that of the second layer. A single, unreversed observation indicated a fourth layer at a depth of about 20 m, but the existence of this layer remains unconfirmed. The observed fundamental mode Love

Con't

DD FORM 1 JAN 73 1473 EDITION OF 1 NOV 65 IS OBSOLETE

Unclassified

SECURITY CLASSIFICATION OF THIS PAGE (When Data Entered)

20. Abstract (Cont'd)

wave dispersion is in agreement with the theoretical dispersion predicted by the refraction velocities. Computed partial derivatives of phase velocity with respect to shear wave velocity show, for the frequencies observed, that the dispersion confirms the thicknesses and velocities of the two upper layers and is not affected by the deeper structure.

PREFACE

This report was written by Donald G. Albert, Geophysicist, of the Geophysical Sciences Branch, Research Division, U.S. Army Cold Regions Research and Engineering Laboratory. This study was funded by DA Project 4A762730AT42, *Design, Construction and Operations Technology for Cold Regions,* Technical Area B, *Combat Development Support,* Technical Effort E, *Environmental Control Methods (USACRREL),* Work Unit 002, *Cold Regions Performance of Seismic-Acoustic Sensor Systems.* Travel support was provided by NATO standardization funds.

The author would like to thank Dr. Roger Turpening of the MIT Lincoln Laboratory for helpful suggestions about adapting the shear wave hammer source technique for use on land, Dr. Robert Herrmann of St. Louis University for providing the computer programs used in the surface wave studies, and Dr. Steven Arcone and Dr. William St. Lawrence of CRREL for technically reviewing the manuscript of this report.

José Llopis operated the seismic recording equipment and also read the P and SH seismograms, providing an independent check of the travel times used in the refraction portion of this report, Charles Miller provided valuable assistance during these experiments, and Perry Smith served as U.S. Field Exercise Team leader during the tests. All of these personnel are with the U.S. Army Engineer Waterways Experiment Station (WES), which also provided the seismic equipment used in these experiments.

CONTENTS

ILLUSTRATIONS

TABLES

SEISMIC SITE CHARACTERIZATION TECHNIQUES APPLIED TO THE NATO RSG-11 TEST SITE IN MÜNSTER NORD, FEDERAL REPUBLIC OF GERMANY

Donald G. Albert

INTRODUCTION

This report presents the results of seismic refraction and surface wave experiments conducted in July and August 1980 at the NATO RSG-11 (Research Study Group) test site in Münster Nord, Federal Republic of Germany. The test site is located in an area of gently undulating glacial till at 52.97°N, 5.16°E (Fig. 1). The experiments were designed to measure the seismic properties of the test site for use in interpreting seismic and acoustic vehicle signatures recorded there during the same time period (NATO 1981). Reversed-refraction profiles of both compressional (P) and shear-horizontal (SH) waves were recorded. The SH records were also used to study the Love wave dispersion curve, providing an independent check of the refraction results. The dispersion curves are of interest since surface waves (including Love and Rayleigh waves) are the strongest seismic waves produced by vehicles.

Seismic refraction techniques were first applied to earthquake records by seismologists studying the large-scale structures of the earth. The Mohorovicic discontinuity separating the crust from the mantle was first detected in 1909, and Gutenberg estimated the depth of the earth's core in 1913 (Bullen 1963). Since that time, the refraction method has been applied to detailed crustal studies, oil prospecting, engineering site studies, and even lunar seismology.

Seismic surface waves are characterized by a propagation path along the earth's surface and displacement amplitudes which decrease rapidly with depth. Both Rayleigh (P-SV coupled) and Love (SH-polarized) surface waves are routinely observed in earthquake studies. Since velocity increases with depth, low frequency waves (with longer wavelengths) penetrate deeper into the earth, travel faster, and arrive at a particular geophone before waves of a higher frequency. Thus a dispersed wave train of low frequencies followed by higher frequencies is observed. Measurements of surface wave velocity as a function of frequency (the Love wave dispersion) from the seismograms are compared to values computed from a theoretical model of seismic velocity and density as a function of depth. Discrepancies are resolved by altering the model. Takeuchi and Saito (1972) provide a complete discussion of the theory of seismic surface waves. Kovach (1978) reviews the use of surface wave dispersion to investigate the properties of the earth's crust.

Although of greater importance to the interpretation of seismic surface waves (and thus vehicle signatures) than P waves, SH waves are much more difficult to measure accurately because of their slower speed (allowing other waves to arrive first) and the lack of a strong SH wave source. Because of these problems and because of the time-consuming field work and interpretation required, SH refraction surveys are

Figure 1. Test site at Münster Nord, FRG. For details on the vehicle signature measurements, see NATO (1981).

rarely undertaken in site surveys. SH waves are used instead of shear-vertical (SV) waves because theoretically no shear-to-compressional-wave conversions exist for this polarization, and because the source itself tends to be less contaminated with P wave motion. Mooney (1976) and Musgrave (1967) provide complete discussions of the refraction technique.

REFRACTION EXPERIMENTS

Procedure

The seismic refraction technique primarily involves measuring the first arrival travel time from source to receiver as the distance (or offset) between them is varied. These travel times can then be analyzed to yield the apparent velocity and depth of refracting layers beneath the refraction line. In general, since velocity tends to increase with depth, records taken at larger offsets will yield the higher velocities characteristic of the deeper layers. If reversed profiles are recorded (i.e. with the source at both ends of the array or spread of receivers), then the data can be used to deduce the true velocity, depth, and dip of the refracting layers.

For this study, we make the usual assumptions that the layers are relatively thick (> 0.1 times the wavelength) and extensive (so that the same refractor is detected over the entire length of the profile), and that the velocity differences between adjacent refractors are large enough to be distinguished by the measurements taken ($\approx$100 m s^{-1} in this case). We also make the assumption in the data analysis that the refractors are plane (though not necessarily horizontal) layers. This assumption is justified by the appearance of straight line segments on the distance vs travel time graphs, and could be relaxed if necessary.

In Figure 2, the ray-path and travel time diagrams are shown for a horizontal two-layer case with constant velocities V_1 and V_2. From Snell's law and the geometry of the figure, the equation for the travel time segment from the second layer (Dobrin 1976) is

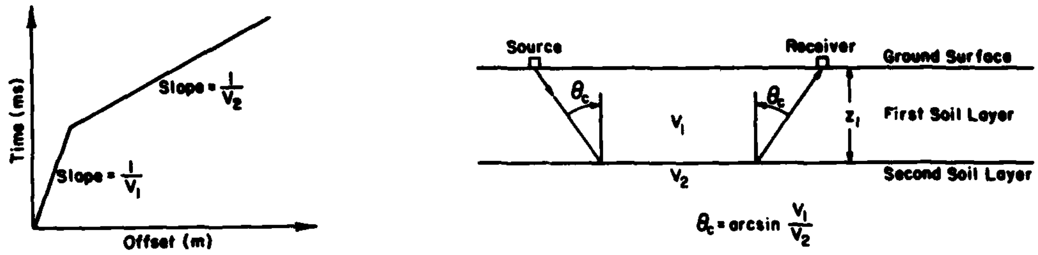

Figure 2. Ray paths and travel time graph for horizontal two-layer case [from Snell's law, θ_c = arcsin (V_1/V_2)]. Adapted from Dobrin (1976).

$$T_2 = \frac{X}{V_2} + (2Z/V_1V_2)\sqrt{V_2^2-V_1^2}$$

where T_2 = the travel time at an offset X for a ray refracted from the second layer
Z = the depth to the second layer
V_i = the velocity of the *i*th layer.

We see that the above equation is a line with a slope of $1/V_2$ and intercept of $(2Z/V_1V_2)\sqrt{V_2^2-V_1^2}$ so that the velocity and depth of the second refracting layer can be determined from the slope and intercept of the travel time graph. This method can be extended to include the more complicated case of multilayered, nonhorizontal media, with a resulting increase in the complexity of the equation of the travel time segment (Knox 1967, Dobrin 1976). The calculation of the velocity and depth of nonhorizontal layers still depends primarily on the values of the slopes and intercepts of the travel time segments.

Equipment

A 12-channel Nimbus ES-1210F signal enhancement seismograph was used to make paper records of the seismograms. This battery-operated seismograph has a 1-k memory for each channel, which can be used to sum individual shots, and has a frequency response of 3 to 800 Hz. No magnetic recording system was available. A geophone spread cable with a 3-m interval between takeouts was used to connect the 12 Mark Products vertical or horizontal component geophones to the seismograph. The natural frequency of the geophones is unknown but is estimated to be 15-20 Hz from the size of the units. Hammer blows were used for the seismic source for all shots.

RESULTS

P waves

P wave reversed refraction measurements were conducted at 11 sites (see Table 1 and Fig. 3). At each location, a short refraction line with 1-m geophone spacing (the overburden, or OB, line) was used to measure the velocity and thickness of the surface material, and a line with a 3-m interval and a 36-m maximum offset was used to measure the deeper layers. At site 2, an additional line with a maximum offset of 63 m was used to penetrate deeper. The P wave lines were all recorded using vertical geophones as receivers and a downward blow from a sledge hammer onto a metal striker plate as the source.

Typical P wave refraction records for site 3 are shown in Figure 4, and the associated travel time graph from the first arrivals is given in Figure 5. Three line segments were fitted by the least-squares method to the travel time graph as shown in the figure. The equations of the line segments were used to calculate the velocities and time intercepts as given in Table 2. The velocity of the surface layer was accurately measured at closer geophone spacings and a value of 203 m s^{-1} was determined. These data were then inverted using a computer program by Mooney (1976) to give the structure along the profile. The measurements indicate that three layers are present with velocities of 203, 502, and 1463 m s^{-1} and with depths to the top of the second and third layers being 1 and 10 m, respectively. Note that the velocity of the deepest layer is quite different from those measured by the individual refraction profiles (1714 and 1277 m s^{-1}). This difference is due to the slight dip of 1.9°. The travel times, graphs, and velocities of all the P wave sites are given in Appendix A.

The most likely interpretation of the P wave

Table 1. P and S wave refraction line parameters.

Line	Type	Direction	Maximum offset (m)	Overburden
1	P	E-W	36	X
2	P	N-S	63	
3	P	N-S	36	
4	P	E-W	36	X
5	P	E-W	36	
6	P	N-S	36	X
7	P	E-W	36	
8	P	N-S	36	X
9	P	E-W	36	
10	P	N-S	36	X
11	P	N-S	36	X
1	SH	E-W	87	X
2	SH	N-S	96	
11	SH	N-S	36	X

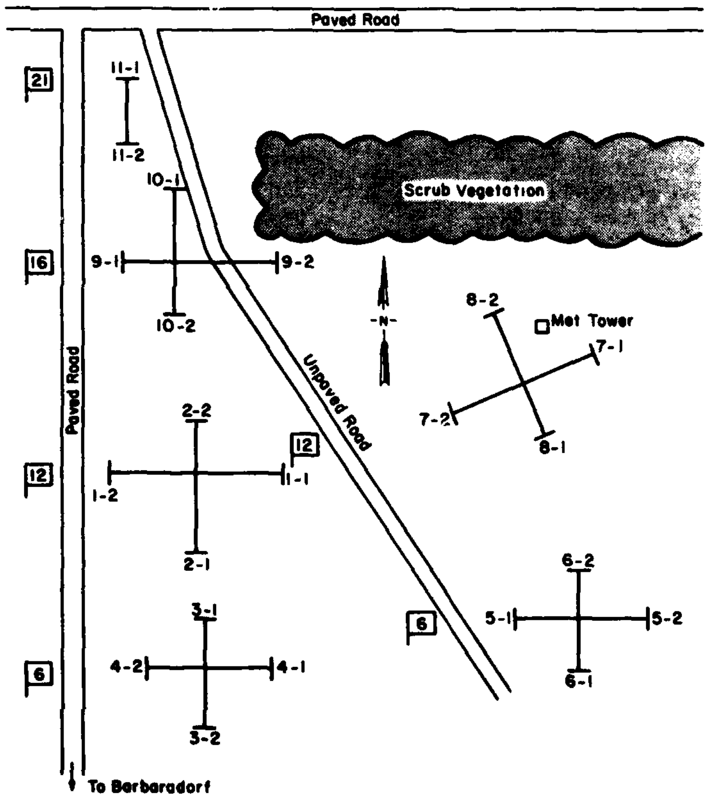

Figure 3. Site map showing the location of the refraction lines.

velocity results at site 3 gives an upper layer composed of unconsolidated glacial till (as also noted from surface and shallow pit observations), underlain by a layer of similar but more compacted material, and then by the water table at a depth of approximately 10 m. Since P waves are usually the first waves to arrive at the geophones, their measurement and interpretation are usually straightforward and are often used in site characterization studies. The very low velocity of the uppermost layer, however, caused some interference between the P wave and the

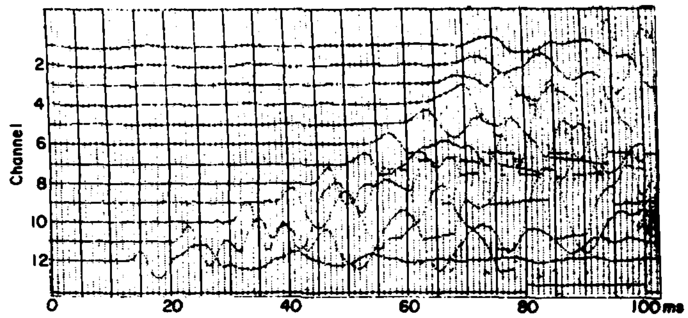

a. *Line 3-1.*

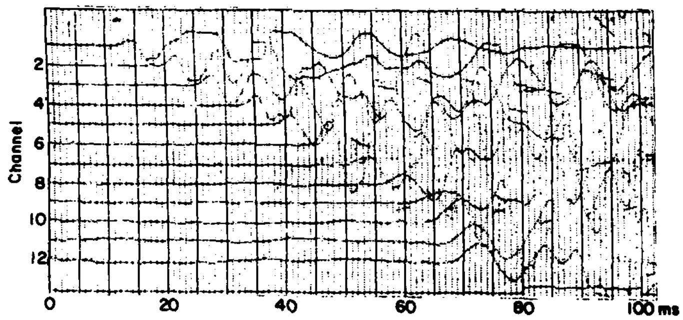

b. *Line 3-2.*

Figure 4. P wave seismic refraction records for line 3.

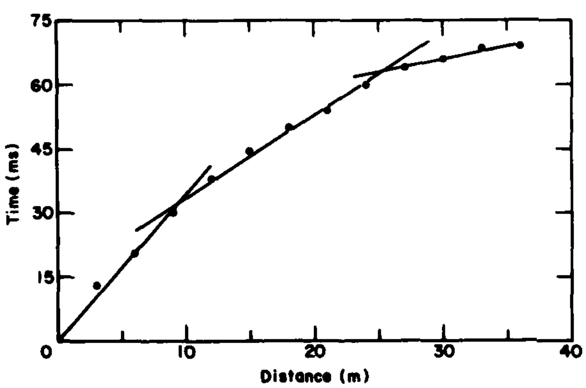

a. *Line 3-1.*

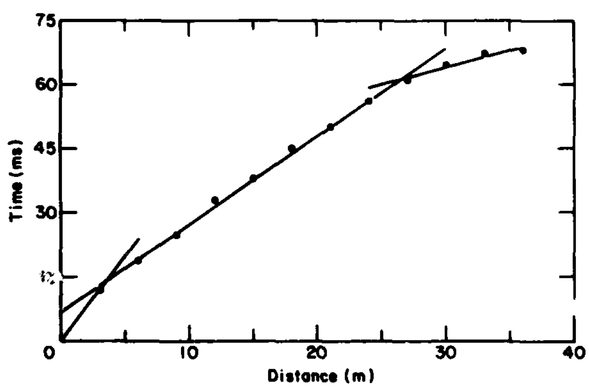

b. *Line 3-2.*

Figure 5. P wave travel time graph for line 3.

sound wave (with a velocity of 330 m s^{-1}). This interference was minimized by covering the metal striker plate with dirt to reduce the strength of the sound wave.

The travel times, graphs, and structures from all the P wave lines are given in Appendix A. The assumptions made in interpreting the data and the inhomogeneity of the medium usually placed the accuracy of the refraction results, when inverted for structure, at about 10%. Thus the results of all the refraction lines are consistent within the range of expected error and can

Table 2. Apparent velocities and final structure from reversed P wave refraction lines at site 3.

Measured characteristics

Layer	Apparent velocity ($m\ s^{-1}$) A†	Apparent velocity ($m\ s^{-1}$) B	Intercept time (ms) A	Intercept time (ms) B
1*	203	203	0.0	0.0
2	516	488	14.1	6.9
3	1714	1277	48.5	40.5

Computed structure**

Layer	Apparent velocity ($m\ s^{-1}$)	Depth (m) A	Depth (m) B	Dip
1	203	1.6	0.8	0.7°
2	502	10.4	9.6	1.9°
3	1463			

*Velocity for layer 1 measured using geophone spacing of 1 m (not shown in Fig. 5).
†Source point A is at north end of refraction line, source point B at south end.
**Accuracy of velocity and depth values is about 10%.

Table 3. P wave velocity structure of the test sites.

Line	V_1^* ($m\ s^{-1}$)	V_2 ($m\ s^{-1}$)	V_3 ($m\ s^{-1}$)	$D_1^\dagger$ (m)	D_2 (m)
1	233	422	1965	0.3	11.0
2		441	1689	0.7	10.5
3		502	1463	1.2	10.0
4	203	487	1315	0.6	9.5
5		472	1394	0.9	9.7
6	217	465	1688	0.7	10.5
7		479		0.7	
8	215	501	1686	0.7	(12.3)**
9		456	1588	0.7	10.5
10	248	456	1663	0.8	11.0
11	310	449	1443	0.6	11.2
Avg.	238	467	1589	0.7	10.3

*V_i = P wave velocity of *i*th layer in $m\ s^{-1}$
† D_i = depth to bottom of the *i*th layer in m.
**D_2 for line 8 is too large because of low velocity zone and was omitted from average (see text).

be generalized to give the model of P wave site characteristics shown in Table 3. The results show that the site is composed of three nearly horizontal layers with the water table at a depth of around 10 m.

Low velocity zone

At sites 7 and 8, the P wave reversed refractions, shown in Figures 6 and 7, are of special interest because of their marked difference from all of the other P wave lines. As shown in Figures 6 and 7, a large delay is present between channels 6 and 7 for line 7-1 (E-W) while line 7-2 appears to show only two layers. The graph for line 8 (Fig. 7) showed similar, but smaller, delays.

These delays are caused by a low velocity zone. Since refracted waves do not exist when a low velocity layer is overlain by a layer of higher velocity [because the critical angle, or angle of refraction, θ_c = arcsin (V_1/V_2) is undefined for V_1

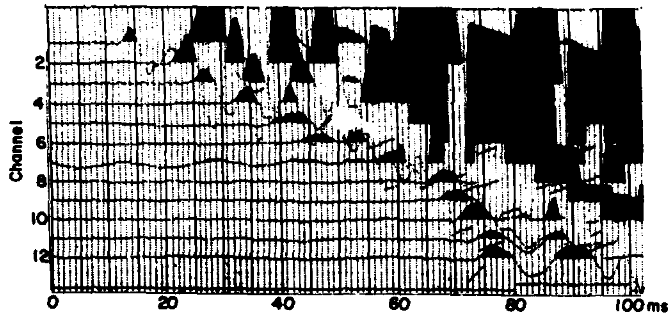

a. Line 7-1.

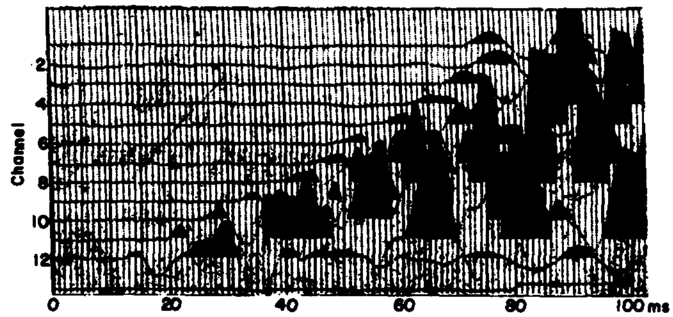

b. Line 7-2.

Figure 6. P wave seismic refraction records for line 7.

$> V_2$], low velocity layers are not directly detected by the seismic refraction method and can only be detected from the delay they cause in arrivals from layers beneath them. The zone at this site is small since the time of arrival at geophone 12 actually precedes that at geophone 11 for shot 7-1, indicating that the path for the ray arriving at channel 12 did not pass through the low velocity area or was less affected by it. A comparison of the travel times between traces for channels 6 and 8 gives a velocity of 286 m s^{-1}, indicating that the low velocity material is similar to the material found on the surface.

Surface observations give supporting evidence for the existence of a low velocity layer. Along line 7, geophones 7 and 8 were placed in a very soft surface layer that was depressed and appeared to be the bottom of a recent puddle. The surface also caved in slightly in places when walked upon. These observations indicate that this location is a natural drainage area and that the increased drainage lowered the seismic velocity of the soil at this spot.

The interpreted results for lines 7 and 8 are in agreement with those for the other locations, but because of the low velocity zone, the refracted rays on line 7 did not penetrate deep enough to detect the water table. Deeper penetration could have been accomplished by increasing the maximum offset. The results for line 8 give a depth of 12.3 m to the water table, which is 2 m greater than the average depth found along the other refraction lines at the test site. This difference can be attributed to the refraction rays traveling through an additional 5 m of low velocity material. By decreasing the geophone spacing and moving the source closer, the low velocity zone could have been accurately mapped.

SH waves

SH wave reversed refraction surveys were conducted along three of the P wave lines at the test site. At present, the best method of producing strong SH waves involves using a horizontally fired mortar as the source (Turpening et al.

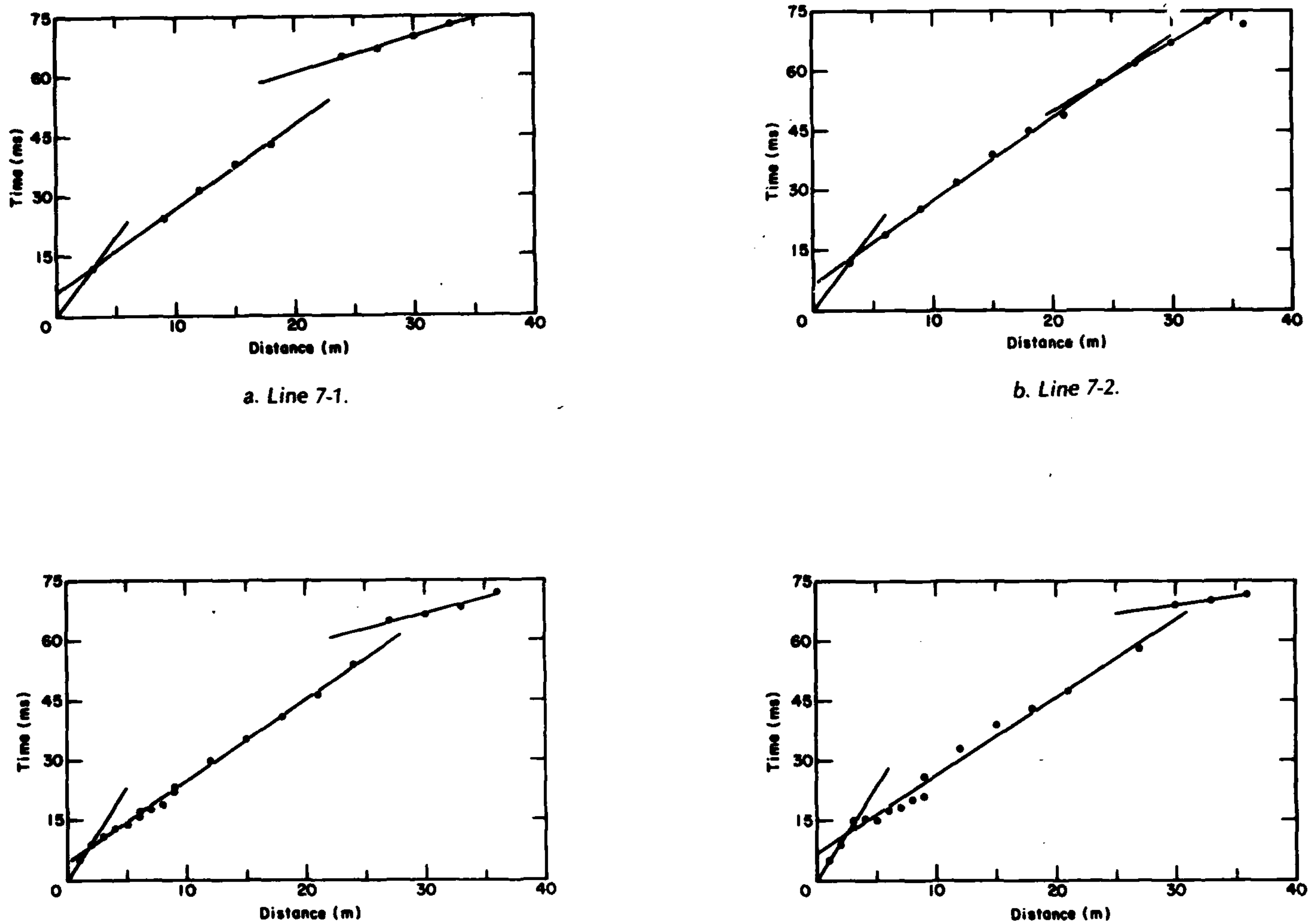

a. Line 7-1.

b. Line 7-2.

c. Line 8-1.

d. Line 8-2.

Figure 7. P wave travel time graphs for lines 7 and 8.

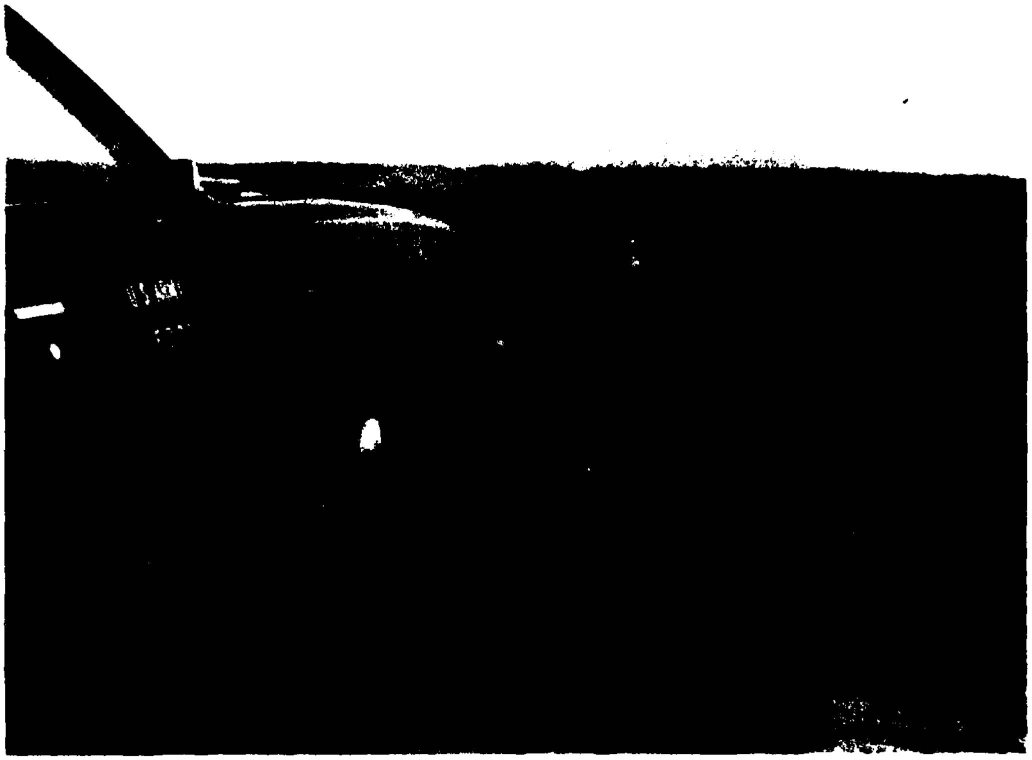

Figure 8. Method of generating SH waves. The sledge hammer is used to strike the board horizontally. A motion-sensitive switch is taped to the handle of the hammer to start the seismic recorder, which is visible in the background.

1980). This technique requires a clear firing range and the use of cement base pads, however, and could not be used for these studies. Instead, sledge hammer blows on the end of a 15- × 15-cm plank held to the ground by the front wheels of a car were used as the source (Fig. 8). Records were taken at each location by hitting both ends of the plank and these records were then compared. Phase relations were used to identify SH waves (the first motion of which reverses with the source polarity) and to eliminate noise from P waves and the acoustic wave (the first motion of which is always away from the source). The hammer technique of SH wave generated has been used by the author and others for shear wave studies in ice sheets (Albert in press).

A pair of SH wave records from line 11 is shown in Figure 9. These records have a geophone spacing of 3 m, with the source located 3 m from the first geophone. The records are identical except that the source polarity is changed from east-to-west (E-W) in Figure 9a to west-to-east (W-E) in Figure 9b. Identification of the shear waves was made by overlaying the two records and picking the earliest arrival exhibiting reversal of phase with the source as shown in Figure 9c. The travel time graph for this location is shown in Figure 10. Additional travel time readings and graphs for other SH refraction sites are given in Appendix B.

The results of the SH wave refractions are listed in Table 4. Because of the weak source, only two layers were detected using SH waves (with the exception of line 1-2). The velocities of the layers were 165 and 276 m s^{-1}, with the top layer about 1.1 m thick. Along line 1-2, a third layer was detected with a velocity of 585 m s^{-1} and a depth of about 20 m. The velocity and depth of this third layer is not accurate, however, since reversed measurements were not obtained.

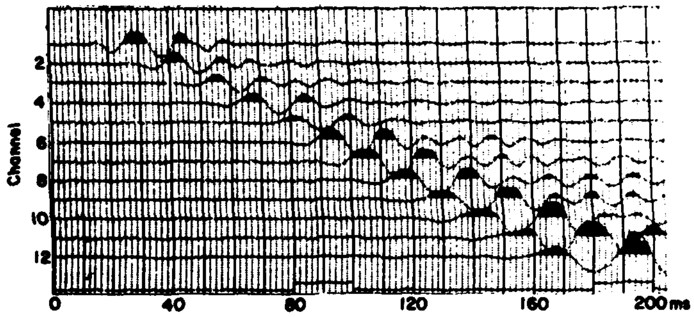

a. Hammer blow at east end of plank (source polarity E to W).

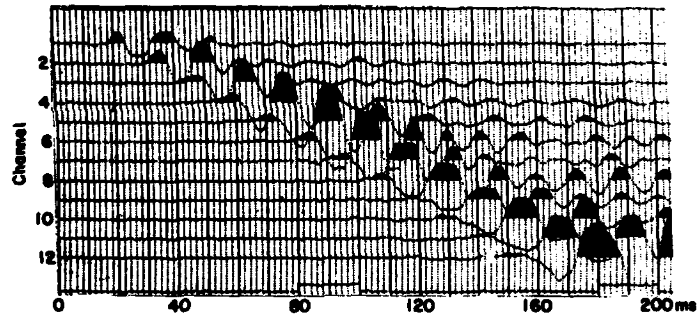

b. Hammer blow at west end of plank (source polarity W to E).

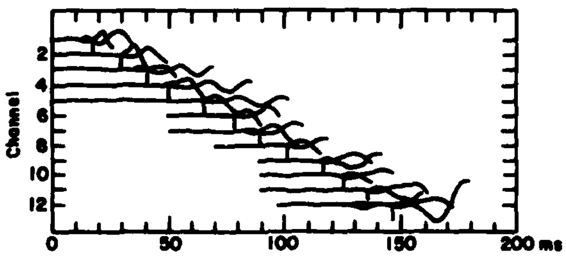

c. Tracing of the two SH wave refraction records in a and b. SH wave arrivals marked with a vertical line below each trace.

Figure 9. SH wave seismic refraction records for line 11-2.

Table 4. SH wave velocity structure of the test site.

Line	V_1^* *(m s⁻¹)*	V_2 *(m s⁻¹)*	V_3 *(m s⁻¹)*	$D_1^\dagger$ *(m)*	D_2^{**} (m)
1	165	278	(585)**	1.3	(20.1)
2	165	291		1.5	
11	166	260		0.6	(20.1)
Average	165	276	(585)	1.1	(20.1)

*V_i = SH wave velocity at *i*th layer in m s^{-1}.
†D_i = Depth to bottom of *i*th layer in m.
**Layer 3 was detected only along one line and was reversed, so these values should be used with caution.

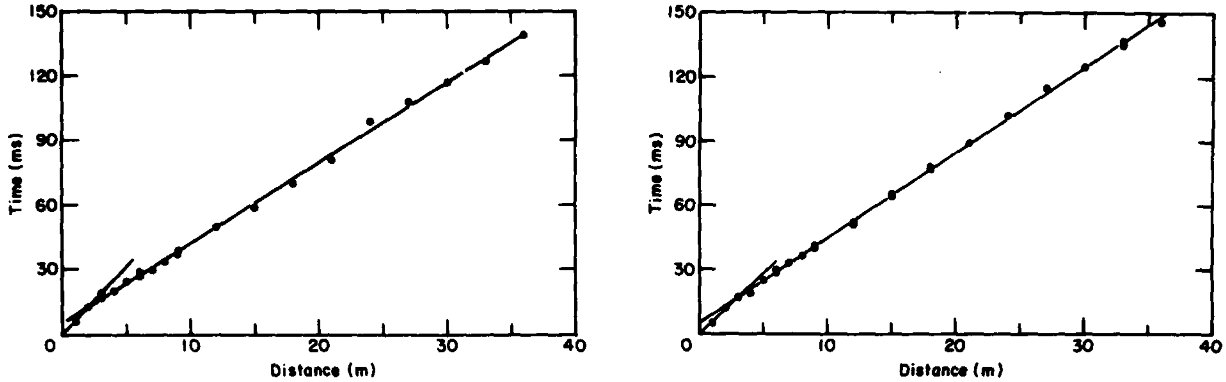

a. *Line 11-1 SH waves.*   b. *Line 11-2 SH waves.*

Figure 10. SH wave travel time graphs.

Table 5. General model of the test site.

Layer	*Depth (m)*	*Thickness (m)*	V_P *(m s^{-1})*	V_{SH} *(m s^{-1})*
1	0.1	1.0	240	165
2	1.0	9.5	470	275
3	10.5	(10.0)*	1590	275*
4	20.5		1590	(585)

*The thickness of layer 3 and the SH velocity of layer 4 are based on a single, unreversed observation.

Note that the SH waves are unaffected by the groundwater table at a depth of 10 m because the shear modulus of a fluid is zero (S waves propagate through the matrix material only). The refracted P waves, however, clearly show the presence of this boundary because the velocity of these waves in water is higher that the velocity of the matrix material.

The general velocity model of the test site derived from refraction experiments is given in Table 5. This model is tested by the analysis of surface wave dispersion presented in the next section.

SURFACE WAVE EXPERIMENTS

Group and phase velocities of Love waves were measured from the SH wave refraction records as a function of frequency. The group velocity or velocity of energy propogation U is related to the phase velocity or velocity of the individual wave crests C by the equation

$$U = C - T\,(dC/dT)$$

where T is the period (see, for example Officer 1974). In practice, it is desirable to fit a theoretical model to observations of both C and U as a function of frequency to provide constraints on the model. Therefore both group and phase velocity functions were investigated in this study. The analysis here will follow the procedures given in Albert (in press). Observed dispersion values for SH refraction records from line 2-2 are listed in Appendix C and are plotted in Figure 11. These records were used because they had the largest offset between the source and the receiver. The Love waves observed on the seismograms had a frequency range of 29 to 43 Hz and phase velocities of 230 to 180 m s^{-1}, corresponding to wavelengths of 8 to 4 m.

Theoretical dispersion curves were calculated using computer programs given by Herrmann (1978). Two theoretical models, listed in Table 6, were used as input to the computer program. Model A is based on the average properties from

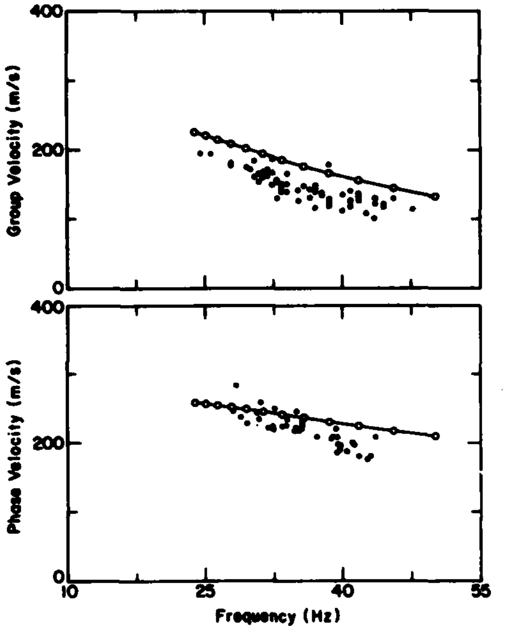

Figure 11. Love wave dispersion (• = observed values along line 2-2, o = values calculated using model A).

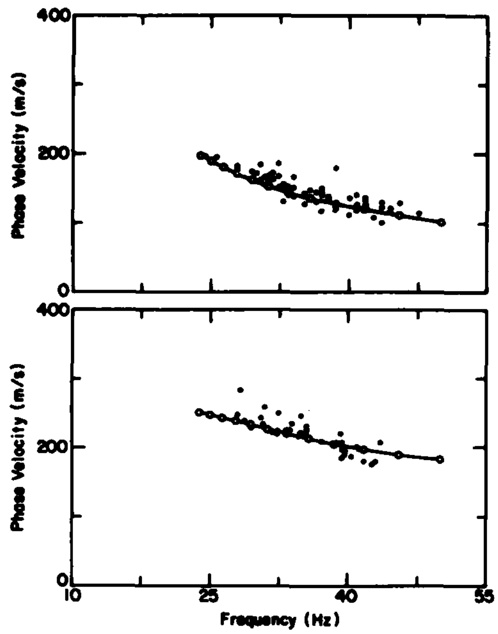

Figure 12. Love wave dispersion (• = observed values along line 2-2, o = values calculated using model B).

Table 6. Theoretical models used to calculate Love wave dispersion.

Thickness (m)	*P velocity ($m\ s^{-1}$)*	*SH velocity ($m\ s^{-1}$)*	*Density ($g\ cm^{-3}$)*
a. Model A, based on the average properties from all refraction lines.			
1.1	238	165	1.9
9.5	467	276	2.0
10.0	1590	276	2.1
∞	1590	585	2.2
b. Model B, based on the properties measured along line 2-2.			
1.1	233	150	1.9
9.5	436	280	2.0
10.0	1590	280	2.1
∞	1590	585	2.2

all of the refraction lines, while model B is based on the properties from line 2-2 only. The density estimates used in the calculations were based on surface measurements.* The densities have very little effect on the theoretical dispersion curves, as increasing the density values by 0.2 did not change the calculated dispersion values.

The theoretical dispersion calculated from model A is plotted along with the observed values in Figure 11. The theoretical group and phase velocities are higher than the observed values. Figure 12 gives a plot of the values calculated using model B, which are in close agreement with the observed dispersion. The agreement between the theoretical and observed surface wave dispersion confirms the refraction velocities measured at this site. The values computed using model A show that the site-to-site velocity variations have measurable effects on the surface wave propagation.

The observed Love wave velocities at this site are very low. Observed group velocities for the frequency range of 25 to 45 Hz were less than 200 m s^{-1}. Because of these low velocities, an acoustic wave produced at the seismic source location will travel faster than the surface waves and interfere with their observations. The air wave will have an especially large effect on the seismic signals generated by noisy, continuous sources such as vehicles.

To show the dependence of the surface wave dispersion on the model parameters, partial derivatives of phase velocity with respect to shear

*C. Miller, USAE Waterways Experiment Station, personal communication, 1980

Table 7. Partial derivatives of phase velocity with respect to shear wave velocity, $\partial C/\partial \beta$, for model B (values of less than 0.01 are omitted from table).

Period (s)	*Frequency (Hz)*	*Depth (m)* 0.0	0.5	1.1	5.8	10.6	15.6	20.9
FIRST MODE								
0.02	50	0.85	0.60	0.12				
0.025	40	0.78	0.70	0.27				
0.035	29	0.44	0.52	0.65	0.01			
0.04	25	0.30	0.38	0.74	0.04			
0.05	20	0.16	0.19	0.74	0.14	0.03		
0.065	15	0.08	0.10	0.64	0.24	0.09	0.02	
0.10	10	0.04	0.05	0.53	0.32	0.17	0.07	
0.20	5	0.03	0.03	0.49	0.42	0.37	0.29	0.09
SECOND MODE								
0.02	50			0.12	0.39	0.41	0.11	
0.025	40		0.01	0.09	0.38	0.45	0.13	
0.035	29	0.01	0.03	0.07	0.35	0.52	0.18	
0.04	25	0.02	0.04	0.09	0.32	0.55	0.22	
0.05	20	0.04	0.06	0.19	0.29	0.58	0.30	0.01
0.10	10	0.02	0.04	0.52	0.76	0.47	0.41	0.69

wave velocities for model B were computed. The values listed in Table 7 show that the shear wave velocities above 6 m control the first mode dispersion curves for the frequency range observed. Thus only the two uppermost velocity layers have been confirmed by the surface wave observations.

SUMMARY AND DISCUSSION

P and SH wave refraction measurements were used to determine the velocity structure of the RSG-11 test site. These measurements show that the area has a nearly horizontal, three-layer structure in the upper 20 m. The velocities and thicknesses of the layers are listed in Table 5.

Love wave dispersion was used to confirm the properties of the two upper layers. The fundamental mode Love waves have observed phase velocities of 180 to 230 m s^{-1} for the frequency range of 43 to 29 Hz. Observed group velocities were less than 200 m s^{-1} for this frequency range, indicating that the direct acoustic wave will have a strong effect on the observation of seismic signals generated by vehicles.

Two methods can be employed in the future to increase the depth of penetration of the surface waves. The first method is to extend the lower bound of the observed frequency range. As seen from Table 7, first mode Love waves in the range from 5 to 20 Hz would provide information on depths up to 20 m. These waves can be recorded by using geophones with a lower natural frequency (4 Hz). The second method, which is more promising because it would provide additional information at all depths, is to use higher mode surface waves. Partial derivatives of phase velocity with respect to shear wave velocity for the second Love wave mode are also shown in Table 6. The dispersion of these waves is controlled by the deeper model parameters. Since the higher mode waves travel at a faster group velocity than those of the fundamental mode, these waves could be recorded by increasing the offsets between the seismic source and the receiver to allow mode separation to occur on the seismograms. Recording the data on magnetic tape would also allow numerical techniques to be used to improve the accuracy of the dispersion observations (Dziewonski and Hales 1972). With the additional information provided by the higher mode surface waves, the resolving power of the data set would be increased enough so that a generalized linear inversion for structural properties would be feasible (Wiggins 1972).

The results of this study have important implications to vehicle signature studies at this site. Since the velocity of the surface layer is very

low, the direct acoustic wave from the vehicle will be a large part of the vehicle signature and will mask the seismic waves from the shallow layers. In addition, strong acoustic-to-seismic coupling will occur, and large amplitude surface waves with phase velocities near that of the speed of sound in air will dominate the signals (Haskell 1951). Using the group velocity curve in Figure 12, the dominant frequency of these air-coupled surface waves (which will travel with a group velocity of 330 m s^{-1}) is extrapolated to be less than 10 Hz.

LITERATURE CITED

Albert, D.G. (in press) Seismic investigations on the Ross Ice Shelf, Antarctica. Submitted to *Antarctic Research Series*. Washington: American Geophysical Union.

Bullen, K.E. (1963) *An Introduction to the Theory of Seismology*. New York: Cambridge University Press.

Dobrin, M.B. (1976) *Introduction to Geophysical Prospecting*. New York: McGraw Hill.

Dziewonski, A.M. and A.L. Hales (1972) Numerical analysis of dispersed seismic waves. In *Methods of Computational Physics* (B.A. Bolt, Ed.). New York: Academic Press, vol. 11, p. 39-85.

Haskell, N.A. (1951) A note on air-coupled surface waves. *Bulletin of the Seismological Society of America*, vol. 41, p. 295-300.

Herrmann, R.B. (1978) *Computer Programs in Earthquake Seismology*. Vol. 2, *Surface Wave Programs*. St. Louis, Missouri: St. Louis University.

Knox, W.A. (1967) Multilayer near-surface refraction computations. In *Seismic Refraction Prospecting* (A.W. Musgrave, Ed.). Society of Exploration Geophysicists, Tulsa, Oklahoma, p. 197-216.

Kovach, R.L. (1978) Seismic surface waves and crustal and upper mantle structure. *Reviews of Geophysics and Space Physics*, vol. 16, p. 1-13.

Mooney, H.M. (1976) *Handbook of Engineering Geophysics*. Minneapolis, Minnesota: Bison Instruments, Inc.

Musgrave, H.W. (1967) *Seismic refraction prospecting*. Society of Exploration Geophysicists, Tulsa, Oklahoma.

NATO (1981) Vehicle signature collection field exercise, summer 1980. North Atlantic Treaty Organization, AC243, Panel III, RSG-11 (NATO Confidential).

Officer, C.B. (1974) *Introduction to Theoretical Geophysics*. New York: Springer-Verlag.

Takeuchi, H. and M. Saito (1972) Seismic surface waves. In *Methods of Computational Physics* (B.A. Bolt, Ed.) New York: Academic Press, vol. 11, p. 217-295.

Turpening, R., R. Stewart, and A. Liskow (1980) A shallow shear wave vertical seismic profiling experiment. Paper presented at the Midwestern SEG Meeting, Tulsa, Oklahoma, March.

Wiggins, R.A. (1972) The general linear inverse problem: Implication of surface waves and free oscillations for earth structure. *Reviews of Geophysics and Space Physics*, vol. 10, p. 251-285.

APPENDIX A: P WAVE REFRACTION DATA

Table A1. Refraction travel times and fitted line segment times.

All distances are in meters. All times are in milliseconds.

X = shot-receiver offset.

T = travel times measured from refraction seismograms.

TLINE = travel time of least-squares line segments fitted to T and X

DIFF = T-TLINE

RSG-11 LINE 1-1 P WAVES

LINE SEGMENT NUMBER 1

X, M	T, MS	TLINE	DIFF
1.0	3.5	2.9	0.6
2.0	5.5	5.9	-0.4
1.0	3.5	2.9	0.6
2.0	5.5	5.9	-0.4
3.0	7.5	8.8	-1.3
3.0	10.5	8.8	1.7
4.0	10.5	11.7	-1.2
4.0	13.0	11.7	1.3
5.0	14.5	14.6	-0.1
5.0	14.5	14.6	-0.1

LINE SEGMENT NUMBER 2

X, M	T, MS	TLINE	DIFF
5.0	14.5	14.5	-0.0
5.0	14.5	14.5	-0.0
6.0	17.0	16.9	0.1
6.0	18.0	16.9	1.1
6.0	17.5	16.9	0.6
7.0	19.0	19.4	-0.4
7.0	19.0	19.4	-0.4
8.0	21.5	21.8	-0.3
8.0	21.5	21.8	-0.3
9.0	24.0	24.2	-0.2
9.0	25.0	24.2	0.8
9.0	23.0	24.2	-1.2
12.0	31.8	31.5	0.3
15.0	38.0	38.8	-0.8
18.0	45.5	46.0	-0.5
21.0	55.0	53.3	1.7
24.0	60.0	60.6	-0.6

LINE SEGMENT NUMBER 3

X, M	T, MS	TLINE	DIFF
24.0	60.0	60.4	-0.4
27.0	63.0	62.6	0.4
30.0	65.0	64.8	0.2
33.0	67.0	67.0	0.0
36.0	69.0	69.2	-0.2

RSG-11 LINE 1-2 P WAVES

LINE SEGMENT NUMBER 1

X, M	T, MS	TLINE	DIFF
1.0	3.5	3.0	0.5
2.0	5.5	6.0	-0.5
3.0	8.0	9.0	-1.0
3.0	9.5	9.0	0.5
3.0	9.5	9.0	0.5

LINE SEGMENT NUMBER 2

X, M	T, MS	TLINE	DIFF
3.0	8.0	8.9	-0.9
3.0	9.5	8.9	0.6
3.0	9.5	8.9	0.6
4.0	12.5	11.2	1.3
5.0	13.5	13.5	-0.0
6.0	16.5	15.8	0.7
6.0	15.0	15.8	-0.8
6.0	17.0	15.8	1.2
7.0	17.5	18.1	-0.6
8.0	20.0	20.4	-0.4
9.0	22.0	22.7	-0.7
9.0	23.0	22.7	0.3
9.0	23.0	22.7	0.3
12.0	29.0	29.5	-0.5
12.0	29.0	29.5	-0.5
15.0	36.0	36.4	-0.4
18.0	40.0	43.2	-3.2
21.0	50.0	50.1	-0.1
21.0	52.0	50.1	1.9
24.0	58.0	57.0	1.0
27.0	64.0	63.8	0.2
27.0	64.0	63.8	0.2

LINE SEGMENT NUMBER 3

X, M	T, MS	TLINE	DIFF
27.0	64.0	63.8	0.2
27.0	64.0	63.8	0.2
30.0	65.0	64.6	0.4
30.0	64.0	64.6	-0.6
33.0	65.0	65.5	-0.5
33.0	65.0	65.5	-0.5
36.0	67.0	66.3	0.7

RSG-11 LINE 2-1 P WAVES

LINE SEGMENT NUMBER 1

X, M	T, MS	TLINE	DIFF
3.0	18.5	15.0	3.5
3.0	13.5	15.0	-1.5
3.0	13.0	15.0	-2.0

LINE SEGMENT NUMBER 2

X, M	T, MS	TLINE	DIFF
3.0	18.5	13.9	4.6
3.0	13.5	13.9	-0.4
3.0	13.0	13.9	-0.9
6.0	21.0	20.6	0.4
6.0	21.0	20.6	0.4
6.0	21.0	20.6	0.4
9.0	26.5	27.4	-0.9
9.0	27.0	27.4	-0.4
9.0	27.0	27.4	-0.4
12.0	33.0	34.1	-1.1
12.0	32.0	34.1	-2.1
12.0	32.0	34.1	-2.1
15.0	39.5	40.9	-1.4
15.0	40.0	40.9	-0.9
15.0	40.0	40.9	-0.9
18.0	49.0	47.6	1.4
18.0	46.0	47.6	-1.6
18.0	48.0	47.6	0.4
21.0	58.0	54.4	3.6
21.0	56.0	54.4	1.6
24.0	62.0	61.1	0.9
24.0	63.0	61.1	1.9
24.0	62.0	61.1	0.9
27.0	67.0	67.8	-0.8
27.0	66.0	67.8	-1.8
27.0	67.0	67.8	-0.8

LINE SEGMENT NUMBER 3

X, M	T, MS	TLINE	DIFF
27.0	67.0	65.7	1.3
27.0	66.0	65.7	0.3
27.0	67.0	65.7	1.3

30.0	68.0	67.4	0.6
30.0	69.0	67.4	1.6
30.0	69.0	67.4	1.6
30.0	66.0	67.4	-1.4
30.0	66.0	67.4	-1.4
33.0	70.0	69.0	1.0
33.0	69.5	69.0	0.5
33.0	70.0	69.0	1.0
33.0	68.0	69.0	-1.0
33.0	67.0	69.0	-2.0
36.0	73.0	70.6	2.4
36.0	73.0	70.6	2.4
36.0	73.0	70.6	2.4
36.0	68.5	70.6	-2.1
36.0	67.0	70.6	-3.6
39.0	70.0	72.3	-2.3
39.0	70.0	72.3	-2.3
42.0	73.0	73.9	-0.9
42.0	73.0	73.9	-0.9
45.0	75.0	75.5	-0.5
45.0	75.0	75.5	-0.5
48.0	78.0	77.1	0.9
48.0	78.0	77.1	0.9
51.0	78.0	78.8	-0.6
51.0	78.0	78.8	-0.8
54.0	80.0	80.4	-0.4
54.0	80.0	80.4	-0.4
57.0	82.0	82.0	-0.0
57.0	83.0	82.0	1.0
60.0	82.0	83.6	-1.6
60.0	85.0	83.6	1.4
63.0	86.0	85.3	0.7
63.0	87.0	85.3	1.7

RSG-11 LINE 2-2 P WAVES

LINE SEGMENT NUMBER 1

X, M	T, MS	TLINE	DIFF
3.0	10.0	10.0	0.0

LINE SEGMENT NUMBER 2

X, M	T, MS	TLINE	DIFF
3.0	10.0	10.5	-0.5
6.0	18.0	17.4	0.6
9.0	23.5	24.2	-0.7
12.0	31.0	31.1	-0.1
15.0	38.0	38.0	0.0
18.0	45.0	44.9	0.1
21.0	53.5	51.8	1.7
24.0	59.0	58.6	0.4
27.0	64.0	65.5	-1.5

LINE SEGMENT NUMBER 3

X, M	T, MS	TLINE	DIFF
27.0	64.0	63.8	0.2
30.0	66.0	65.7	0.3
30.0	64.5	65.7	-1.2
33.0	68.0	67.6	0.4
33.0	66.0	67.6	-1.6
36.0	71.0	69.5	1.5
36.0	69.0	69.5	-0.5
39.0	71.0	71.5	-0.5
42.0	74.0	73.4	0.6
45.0	77.0	75.3	1.7
48.0	78.0	77.2	0.8
51.0	79.5	79.2	0.3
54.0	80.0	81.1	-1.1
57.0	82.0	83.0	-1.0

60.0	86.0	84.9	1.1
63.0	86.0	86.9	-0.9

RSG-11 LINE 3-1 P WAVES

LINE SEGMENT NUMBER 1

X, M	T, MS	TLINE	DIFF
0.0	0.0	0.0	-0.0
3.0	13.0	10.3	2.7
6.0	20.5	20.6	-0.1
9.0	30.0	30.9	-0.9

LINE SEGMENT NUMBER 2

X, M	T, MS	TLINE	DIFF
9.0	30.0	31.5	-1.5
12.0	38.0	37.4	0.6
15.0	44.5	43.2	1.3
18.0	50.0	49.0	1.0
21.0	54.0	54.8	-0.8
24.0	60.0	60.6	-0.6

LINE SEGMENT NUMBER 3

X, M	T, MS	TLINE	DIFF
27.0	64.0	64.2	-0.2
30.0	66.0	66.0	0.0
33.0	68.5	67.7	0.8
36.0	69.0	69.5	-0.5

RSG-11 LINE 3-2 P WAVES

LINE SEGMENT NUMBER 1

X, M	T, MS	TLINE	DIFF
3.0	12.0	12.0	0.0

LINE SEGMENT NUMBER 2

X, M	T, MS	TLINE	DIFF
3.0	12.0	13.1	-1.1
6.0	19.0	19.2	-0.2
9.0	25.0	25.4	-0.4
12.0	33.0	31.5	1.5
15.0	38.0	37.7	0.3
18.0	45.0	43.8	1.2
21.0	50.0	50.0	0.0
24.0	56.0	56.1	-0.1
27.0	61.0	62.3	-1.3

LINE SEGMENT NUMBER 3

X, M	T, MS	TLINE	DIFF
27.0	61.0	61.6	-0.6
30.0	64.5	63.9	0.6
33.0	67.0	66.3	0.7
36.0	68.0	68.6	-0.6

RSG-11 LINE 4-1 P WAVES

LINE SEGMENT NUMBER 1

X, M	T, MS	TLINE	DIFF
0.0	0.0	0.0	-0.0
1.0	6.0	5.2	0.8
2.0	10.0	10.4	-0.4

LINE SEGMENT NUMBER 2

X, M	T, MS	TLINE	DIFF
3.0	11.0	11.9	-0.9
6.0	17.0	18.2	-1.2
9.0	23.0	24.5	-1.5
12.0	29.0	30.8	-1.8
15.0	36.0	37.1	-1.1
18.0	42.0	43.4	-1.4
21.0	50.0	49.7	0.3
24.0	58.0	56.0	2.0
2.0	10.0	9.8	0.2
3.0	13.0	11.9	1.1
5.0	17.0	16.1	0.9
6.0	20.0	18.2	1.8
7.0	20.5	20.3	0.2
8.0	23.0	22.4	0.6
9.0	25.0	24.5	0.5

LINE SEGMENT NUMBER 3

X, M	T, MS	TLINE	DIFF
24.0	58.0	57.6	0.4
27.0	60.0	60.4	-0.4
30.0	63.0	63.2	-0.2
33.0	66.0	66.0	0.0
36.0	69.0	68.8	0.2

RSG-11 LINE 4-2 P WAVES

LINE SEGMENT NUMBER 1

X, M	T, MS	TLINE	DIFF
0.0	0.0	-0.0	0.0
1.0	4.5	4.7	-0.2
2.0	9.5	9.4	0.1

LINE SEGMENT NUMBER 2

X, M	T, MS	TLINE	DIFF
3.0	11.5	11.9	-0.4
6.0	19.0	18.0	1.0
9.0	24.0	24.0	0.0
12.0	30.0	30.0	-0.0
15.0	36.0	36.0	-0.0
18.0	42.0	42.1	-0.1
21.0	48.0	48.1	-0.1
24.0	53.5	54.1	-0.6
27.0	60.5	60.2	0.3
2.0	9.5	9.9	-0.4
3.0	11.0	11.9	-0.9
4.0	14.0	13.9	0.1
5.0	16.0	15.9	0.1
6.0	18.0	18.0	0.0
7.0	20.5	20.0	0.5
8.0	22.5	22.0	0.5
9.0	24.0	24.0	0.0

LINE SEGMENT NUMBER 3

X, M	T, MS	TLINE	DIFF
27.0	60.5	60.2	0.3
30.0	62.0	62.0	0.0
33.0	63.0	63.7	-0.7
36.0	66.0	65.5	0.5

RSG-11 LINE 5-1 P WAVES

LINE SEGMENT NUMBER 1

X, M	T, MS	TLINE	DIFF
3.0	14.0	14.0	0.0

LINE SEGMENT NUMBER 2

X, M	T, MS	TLINE	DIFF
3.0	14.0	14.2	-0.2
6.0	21.0	20.5	0.5
9.0	27.5	26.8	0.7
12.0	33.0	33.1	-0.1
15.0	39.0	39.4	-0.4
18.0	44.0	45.7	-1.7
21.0	52.5	52.0	0.5
24.0	59.0	58.2	0.8

LINE SEGMENT NUMBER 3

X, M	T, MS	TLINE	DIFF
24.0	59.0	59.2	-0.2
27.0	62.0	61.5	0.5
30.0	64.0	63.8	0.2
33.0	65.0	66.1	-1.1
36.0	69.0	68.4	0.6

RSG-11 LINE 5-2 P WAVES

LINE SEGMENT NUMBER 1

X, M	T, MS	TLINE	DIFF
3.0	12.0	12.0	0.0

LINE SEGMENT NUMBER 2

X, M	T, MS	TLINE	DIFF
3.0	12.0	12.4	-0.4
6.0	19.0	18.8	0.2
9.0	25.5	25.2	0.3
12.0	31.0	31.6	-0.6
15.0	39.0	38.1	0.9
18.0	44.0	44.5	-0.5
21.0	51.0	50.9	0.1
24.0	57.5	57.3	0.2
27.0	63.5	63.8	-0.3

LINE SEGMENT NUMBER 3

X, M	T, MS	TLINE	DIFF
27.0	63.5	63.0	0.5
30.0	64.5	65.0	-0.5
33.0	66.5	67.0	-0.5
36.0	69.5	69.0	0.5

RSG-11 LINE 6-1 P WAVES

LINE SEGMENT NUMBER 1

X, M	T, MS	TLINE	DIFF
0.0	0.0	0.0	-0.0
1.0	6.5	5.1	1.4
2.0	9.5	10.2	-0.7

LINE SEGMENT NUMBER 2

X, M	T, MS	TLINE	DIFF
3.0	11.5	12.0	-0.5
6.0	17.5	18.2	-0.7

9.0	24.0	24.5	-0.5
12.0	31.0	30.8	0.2
15.0	38.0	37.1	0.9
18.0	44.0	43.3	0.7
21.0	49.0	49.6	-0.6
24.0	56.0	55.9	0.1
27.0	61.5	62.2	-0.7
2.0	9.5	9.9	-0.4
3.0	12.0	12.0	0.0
4.0	14.0	14.0	-0.0
5.0	16.0	16.1	-0.1
6.0	18.5	18.2	0.3
7.0	21.0	20.3	0.7
8.0	23.0	22.4	0.6
9.0	24.5	24.5	-0.0

LINE SEGMENT NUMBER 3

X, M	T, MS	TLINE	DIFF
27.0	61.5	61.9	-0.4
30.0	64.5	63.9	0.6
33.0	66.0	65.8	0.2
36.0	67.5	67.8	-0.3

RSG-11 LINE 6-2 P WAVES

LINE SEGMENT NUMBER 1

X, M	T, MS	TLINE	DIFF
0.0	0.0	-0.0	0.0
1.0	4.0	4.2	-0.2
2.0	8.5	8.4	0.1

LINE SEGMENT NUMBER 2

X, M	T, MS	TLINE	DIFF
3.0	12.0	12.1	-0.1
6.0	19.5	18.7	0.8
9.0	26.0	25.3	0.7
12.0	32.0	32.0	0.0
15.0	41.0	38.6	2.4
18.0	47.0	45.2	1.8
21.0	52.0	51.8	0.2
24.0	58.0	58.4	-0.4
27.0	63.0	65.1	-2.1
2.0	8.5	9.9	-1.4
3.0	11.8	12.1	-0.4
4.0	14.5	14.3	0.2
5.0	16.5	16.5	-0.0
6.0	18.5	18.7	-0.2
7.0	21.0	20.9	0.1
8.0	22.5	23.1	-0.6
9.0	24.5	25.3	-0.8

LINE SEGMENT NUMBER 3

X, M	T, MS	TLINE	DIFF
27.0	63.0	63.1	-0.1
30.0	65.0	64.7	0.3
33.0	66.0	66.3	-0.3
36.0	68.0	67.9	0.1

RSG-11 LINE 7-1 P WAVES

LINE SEGMENT NUMBER 1

X, M	T, MS	TLINE	DIFF
3.0	12.0	12.0	0.0

LINE SEGMENT NUMBER 2

X, M	T, MS	TLINE	DIFF
3.0	12.0	12.1	-0.1
9.0	24.5	24.8	-0.3
12.0	31.5	31.1	0.4
15.0	38.0	37.4	0.6
18.0	43.0	43.7	-0.7

LINE SEGMENT NUMBER 3

X, M	T, MS	TLINE	DIFF
24.0	65.0	64.7	0.3
27.0	67.0	67.4	-0.4
30.0	70.0	70.1	-0.1
33.0	73.0	72.8	0.2

RSG-11 LINE 7-2 P WAVES

LINE SEGMENT NUMBER 1

X, M	T, MS	TLINE	DIFF
0.0	0.0	0.0	0.0
3.0	12.0	12.0	0.0

LINE SEGMENT NUMBER 2

X, M	T, MS	TLINE	DIFF
3.0	12.0	12.9	-0.9
6.0	19.0	19.1	-0.1
9.0	25.5	25.4	0.1
12.0	32.0	31.6	0.4
15.0	39.0	37.8	1.2
18.0	45.0	44.1	0.9
21.0	49.0	50.3	-1.3
24.0	57.0	56.5	0.5
27.0	62.0	62.8	-0.8

LINE SEGMENT NUMBER 3

X, M	T, MS	TLINE	DIFF
27.0	62.0	61.9	0.1
30.0	67.0	67.2	-0.2
33.0	72.5	72.4	0.1

RSG-11 LINE 8-1 P WAVES

LINE SEGMENT NUMBER 1

X, M	T, MS	TLINE	DIFF
0.0	0.0	0.0	-0.0
1.0	5.3	4.7	0.6
2.0	9.0	9.3	-0.3

LINE SEGMENT NUMBER 2

X, M	T, MS	TLINE	DIFF
3.0	11.0	10.6	0.4
6.0	16.0	16.7	-0.7
9.0	23.5	22.8	0.7
12.0	30.0	28.9	1.1
15.0	35.5	35.0	0.5
18.0	41.0	41.1	-0.1
21.0	46.5	47.3	-0.8
24.0	54.0	53.4	0.6
2.0	9.0	8.5	0.5
3.0	11.0	10.6	0.4
4.0	13.0	12.6	0.4

5.0	14.0	14.6	-0.6
6.0	17.3	16.7	0.6
7.0	18.0	18.7	-0.7
8.0	19.0	20.8	-1.8
9.0	22.3	22.8	-0.5

LINE SEGMENT NUMBER 3

X, M	T, MS	TLINE	DIFF
27.0	65.0	64.5	0.5
30.0	66.5	66.8	-0.3
33.0	68.5	69.1	-0.6
36.0	72.0	71.4	0.6

RSG-11 LINE 8-2 P WAVES

LINE SEGMENT NUMBER 1

X, M	T, MS	TLINE	DIFF
0.0	0.0	0.0	-0.0
3.0	15.0	14.1	0.9
1.0	5.0	4.7	0.3
2.0	9.0	9.4	-0.4
3.0	13.3	14.1	-0.8

LINE SEGMENT NUMBER 2

X, M	T, MS	TLINE	DIFF
3.0	15.0	12.7	2.3
9.0	26.0	24.4	1.6
12.0	33.0	30.2	2.8
15.0	39.0	36.1	2.9
18.0	43.0	41.9	1.1
21.0	47.5	47.8	-0.3
27.0	58.0	59.5	-1.5
3.0	13.3	12.7	0.6
4.0	15.5	14.6	0.9
5.0	15.0	16.6	-1.6
6.0	17.5	18.5	-1.0
7.0	18.3	20.5	-2.2
8.0	20.3	22.4	-2.2
9.0	21.0	24.4	-3.4

LINE SEGMENT NUMBER 3

X, M	T, MS	TLINE	DIFF
30.0	69.0	68.9	0.1
33.0	70.0	70.2	-0.2
36.0	71.5	71.4	0.1

RSG-11 LINE 9-1 P WAVES

LINE SEGMENT NUMBER 1

X, M	T, MS	TLINE	DIFF
3.0	11.0	11.0	0.0

LINE SEGMENT NUMBER 2

X, M	T, MS	TLINE	DIFF
3.0	11.0	11.9	-0.9
6.0	19.0	18.3	0.7
9.0	25.5	24.8	0.7
12.0	31.5	31.3	0.2
15.0	38.0	37.7	0.3
18.0	44.0	44.2	-0.2
21.0	49.0	50.6	-1.6
24.0	57.0	57.1	-0.1
27.0	64.5	63.6	0.9

LINE SEGMENT NUMBER 3

X, M	T, MS	TLINE	DIFF
27.0	64.5	63.5	1.0
30.0	64.0	65.0	-1.0
33.0	65.8	66.6	-0.8
36.0	69.0	68.1	0.9

RSG-11 LINE 9-2 P WAVES

LINE SEGMENT NUMBER 1

X, M	T, MS	TLINE	DIFF
3.0	12.5	12.5	0.0

LINE SEGMENT NUMBER 2

X, M	T, MS	TLINE	DIFF
3.0	12.5	11.1	1.4
6.0	17.0	17.8	-0.8
9.0	23.5	24.5	-1.0
12.0	31.5	31.2	0.3
15.0	37.5	37.9	-0.4
18.0	44.0	44.6	-0.6
21.0	52.5	51.3	1.2
24.0	59.5	58.0	1.5
27.0	63.5	64.7	-1.2

LINE SEGMENT NUMBER 3

X, M	T, MS	TLINE	DIFF
27.0	63.5	64.0	-0.5
30.0	67.0	66.3	0.8
33.0	68.5	68.5	0.0
36.0	70.5	70.8	-0.3

RSG-11 LINE 10-1 P WAVES

LINE SEGMENT NUMBER 1

X, M	T, MS	TLINE	DIFF
0.0	0.0	-0.0	0.0
3.0	11.5	10.7	0.8
1.0	3.0	3.6	-0.6
2.0	7.0	7.2	-0.2
3.0	10.3	10.7	-0.5

LINE SEGMENT NUMBER 2

X, M	T, MS	TLINE	DIFF
3.0	11.5	11.4	0.1
6.0	16.5	17.9	-1.4
9.0	24.0	24.4	-0.4
12.0	29.0	30.9	-1.9
18.0	44.0	43.9	0.1
21.0	50.0	50.5	-0.5
24.0	57.0	57.0	0.0
27.0	64.0	63.5	0.5
3.0	10.3	11.4	-1.1
4.0	13.5	13.5	-0.0
5.0	16.8	15.7	1.0
6.0	19.0	17.9	1.1
8.0	23.0	22.2	0.8
9.0	26.0	24.4	1.6

LINE SEGMENT NUMBER 3

X, M	T, MS	TLINE	DIFF
27.0	64.0	64.7	-0.7
30.0	68.0	66.9	1.1
33.0	69.0	69.1	-0.1
36.0	71.0	71.3	-0.3

RSG-11 LINE 10-2 P WAVES

LINE SEGMENT NUMBER 1

X, M	T, MS	TLINE	DIFF
0.0	0.0	-0.0	0.0
1.0	4.0	4.6	-0.6
2.0	9.5	9.2	0.3

LINE SEGMENT NUMBER 2

X, M	T, MS	TLINE	DIFF
3.0	12.0	12.2	-0.2
6.0	18.5	18.9	-0.4
9.0	26.0	25.5	0.5
12.0	32.5	32.1	0.4
15.0	39.0	38.8	0.2
18.0	45.0	45.4	-0.4
21.0	51.5	52.1	-0.6
24.0	58.0	58.7	-0.7
27.0	66.0	65.4	0.6
2.0	9.5	10.0	-0.5
3.0	11.5	12.2	-0.7
4.0	15.0	14.4	0.6
5.0	16.5	16.6	-0.1
6.0	18.5	18.9	-0.4
7.0	21.5	21.1	0.4
8.0	24.0	23.3	0.7
9.0	26.0	25.5	0.5

LINE SEGMENT NUMBER 3

X, M	T, MS	TLINE	DIFF
27.0	66.0	65.9	0.1
30.0	67.5	67.3	0.2
33.0	68.0	68.7	-0.7
36.0	70.5	70.1	0.4

RSG-11 TEST SITE LINE 11-1 P WAVES

LINE SEGMENT NUMBER 1

X, M	T, MS	TLINE	DIFF
1.0	3.0	3.2	-0.2
2.0	7.0	6.5	0.5
3.0	9.5	9.7	-0.2
3.0	10.0	9.7	0.3
4.0	12.8	13.0	-0.2

LINE SEGMENT NUMBER 2

X, M	T, MS	TLINE	DIFF
4.0	12.8	11.5	1.3
5.0	14.0	13.6	0.4
6.0	15.0	15.8	-0.8
6.0	15.0	15.8	-0.8
7.0	18.5	17.9	0.6
8.0	20.5	20.1	0.4
9.0	22.5	22.2	0.3
9.0	22.0	22.2	-0.2
12.0	28.0	28.7	-0.7
15.0	34.5	35.1	-0.6
18.0	41.0	41.6	-0.6
21.0	48.0	48.0	-0.0
24.0	54.0	54.5	-0.5
27.0	61.5	60.9	0.6
30.0	68.0	67.4	0.6

LINE SEGMENT NUMBER 3

X, M	T, MS	TLINE	DIFF
30.0	68.0	67.9	0.1
33.0	69.0	69.2	-0.2
36.0	70.5	70.4	0.1

RSG-11 TEST SITE LINE 11-2 P WAVES

LINE SEGMENT NUMBER 1

X, M	T, MS	TLINE	DIFF
1.0	4.0	3.2	0.8
2.0	6.5	6.4	0.1
3.0	9.8	9.7	0.1
3.0	9.5	9.7	-0.2
4.0	12.8	12.9	-0.1

LINE SEGMENT NUMBER 2

X, M	T, MS	TLINE	DIFF
4.0	12.8	12.8	-0.0
5.0	15.0	15.1	-0.1
6.0	17.5	17.3	0.2
6.0	17.0	17.3	-0.3
7.0	20.0	19.6	0.4
8.0	22.0	21.9	0.1
9.0	26.0	24.1	1.9
9.0	23.8	24.1	-0.4
12.0	30.5	30.9	-0.4
15.0	36.0	37.7	-1.7
18.0	44.0	44.5	-0.5
21.0	50.0	51.3	-1.3
24.0	60.0	58.1	1.9
27.0	65.0	64.9	0.1

LINE SEGMENT NUMBER 3

X, M	T, MS	TLINE	DIFF
27.0	65.0	65.4	-0.4
30.0	67.5	67.3	0.2
33.0	70.0	69.2	0.8
36.0	70.5	71.1	-0.6

RSG-11 LINE 11-1 P WAVE PEAKS

LINE SEGMENT NUMBER 3

X, M	T, MS	TLINE	DIFF
30.0	72.0	71.8	0.3
33.0	73.0	74.0	-1.0
33.0	74.5	74.0	0.5
36.0	75.5	76.2	-0.7
36.0	77.3	76.2	1.0

Table A2. Fitted line segments. Characteristics of the line segments which were fitted to the data are listed for all lines.

NPTS = no. of data points
(XMIN, XMAX) = interval of line segment
MSE = mean square error = $(1/NPTS) \cdot \sqrt{\Sigma (T\text{-}TLINE)^2}$

RSG-11 LINE 1-1 P WAVES

SEGMENT NO.	XMIN M	XMAX M	NPTS	VELOCITY M/S	INTERCEPT TIME, MS	MSE MS	CORREL COEFF
1	0.0	5.0	10	342.	0.0	0.3	0.9909
2	5.0	24.0	17	412.	2.4	0.2	0.9974
3	24.0	36.0	5	1364.	42.8	0.1	0.9918

RSG-11 LINE 1-2 P WAVES

SEGMENT NO.	XMIN M	XMAX M	NPTS	VELOCITY M/S	INTERCEPT TIME, MS	MSE MS	CORREL COEFF
1	0.0	3.0	5	335.	0.0	0.3	0.9931
2	3.0	27.0	22	437.	2.1	0.2	0.9967
3	27.0	36.0	7	3545.	56.2	0.2	0.7754

RSG-11 LINE 2-1 P WAVES

SEGMENT NO.	XMIN M	XMAX M	NPTS	VELOCITY M/S	INTERCEPT TIME, MS	MSE MS	CORREL COEFF
1	0.0	3.0	3	200.	0.0	1.4	0.9733
2	3.0	27.0	26	445.	7.2	0.3	0.9916
3	27.0	63.0	36	1844.	51.1	0.2	0.9440

RSG-11 LINE 2-2 P WAVES

SEGMENT NO.	XMIN M	XMAX M	NPTS	VELOCITY M/S	INTERCEPT TIME, MS	MSE MS	CORREL COEFF
1	0.0	3.0	1	300.	-0.0	0.0	1.0000
2	3.0	27.0	9	436.	3.6	0.3	0.9977
3	27.0	63.0	16	1559.	46.5	0.2	0.9822

RSG-11 LINE 3-1 P WAVES

SEGMENT NO.	XMIN M	XMAX M	NPTS	VELOCITY M/S	INTERCEPT TIME, MS	MSE MS	CORREL COEFF
1	0.0	9.0	4	292.	0.0	0.7	0.9946
2	9.0	26.0	6	516.	14.1	0.4	0.9890
3	26.0	36.0	4	1714.	48.5	0.2	0.9459

RSG-11 LINE 3-2 P WAVES

SEGMENT NO.	XMIN M	XMAX M	NPTS	VELOCITY M/S	INTERCEPT TIME, MS	MSE MS	CORREL COEFF
1	0.0	3.0	1	250.	-0.0	0.0	1.0000
2	3.0	27.0	9	488.	6.9	0.3	0.9971
3	27.0	36.0	4	1277.	40.4	0.3	0.9460

RSG-11 LINE 4-1 P WAVES

SEGMENT NO.	XMIN M	XMAX M	NPTS	VELOCITY M/S	INTERCEPT TIME, MS	MSE MS	CORREL COEFF
1	0.0	2.0	3	192.	0.0	0.3	0.9941
2	2.0	24.0	15	476.	5.6	0.3	0.9927
3	24.0	36.0	5	1071.	35.2	0.1	0.9949

RSG-11 LINE 4-2 P WAVES

SEGMENT NO.	XMIN M	XMAX M	NPTS	VELOCITY M/S	INTERCEPT TIME, MS	MSE MS	CORREL COEFF
1	0.0	2.0	3	213.	-0.0	0.1	0.9995
2	2.0	27.0	17	498.	5.9	0.1	0.9991
3	27.0	36.0	4	1714.	44.5	0.2	0.9459

RSG-11 LINE 5-1 P WAVES

SEGMENT NO.	XMIN M	XMAX M	NPTS	VELOCITY M/S	INTERCEPT TIME, MS	MSE MS	CORREL COEFF
1	0.0	3.0	1	214.	-0.0	0.0	1.0000
2	3.0	24.0	8	477.	8.0	0.3	0.9973
3	24.0	36.0	5	1304.	40.8	0.3	0.9653

RSG-11 LINE 5-2 P WAVES

SEGMENT NO.	XMIN M	XMAX M	NPTS	VELOCITY M/S	INTERCEPT TIME, MS	MSE MS	CORREL COEFF
1	0.0	3.0	1	250.	-0.0	0.0	1.0000
2	3.0	27.0	9	467.	5.9	0.2	0.9992
3	27.0	36.0	4	1500.	45.0	0.2	0.9524

RSG-11 LINE 6-1 P WAVES

SEGMENT NO.	XMIN M	XMAX M	NPTS	VELOCITY M/S	INTERCEPT TIME, MS	MSE MS	CORREL COEFF
1	0.0	2.0	3	196.	0.0	0.5	0.9815
2	2.0	27.0	17	478.	5.7	0.1	0.9990
3	27.0	36.0	4	1538.	44.4	0.2	0.9657

RSG-11 LINE 6-2 P WAVES

SEGMENT NO.	XMIN M	XMAX M	NPTS	VELOCITY M/S	INTERCEPT TIME, MS	MSE MS	CORREL COEFF
1	0.0	2.0	3	238.	-0.0	0.1	0.9994
2	2.0	27.0	17	453.	5.5	0.2	0.9962
3	27.0	36.0	4	1875.	48.7	0.1	0.9846

RSG-11 LINE 7-1 P WAVES

SEGMENT NO.	XMIN M	XMAX M	NPTS	VELOCITY M/S	INTERCEPT TIME, MS	MSE MS	CORREL COEFF
1	0.0	3.0	1	250.	-0.0	0.0	1.0000
2	3.0	20.0	5	476.	5.8	0.2	0.9981
3	20.0	36.0	4	1111.	43.1	0.1	0.9918

RSG-11 LINE 7-2 P WAVES

SEGMENT NO.	XMIN M	XMAX M	NPTS	VELOCITY M/S	INTERCEPT TIME, MS	MSE MS	CORREL COEFF
1	0.0	3.0	2	250.	0.0	0.0	1.0000
2	3.0	27.0	9	481.	6.7	0.3	0.9975
3	27.0	33.0	3	571.	14.7	0.1	0.9992

RG-11 LINE 8-1 P WAVES

SEGMENT NO.	XMIN M	XMAX M	NPTS	VELOCITY M/S	INTERCEPT TIME, MS	MSE MS	CORREL COEFF
1	0.0	2.0	3	215.	0.0	0.2	0.9959
2	2.0	25.0	16	490.	4.4	0.2	0.9969
3	25.0	36.0	4	1304.	43.8	0.3	0.9618

RSG-11 LINE 8-2 P WAVES

SEGMENT NO.	XMIN M	XMAX M	NPTS	VELOCITY M/S	INTERCEPT TIME, MS	MSE MS	CORREL COEFF
1	0.0	3.0	5	213.	0.0	0.3	0.9965
2	3.0	28.0	14	513.	6.8	0.5	0.9800
3	28.0	36.0	3	2400.	56.4	0.1	0.9865

RSG-11 LINE 9-1 P WAVES

SEGMENT NO.	XMIN M	XMAX M	NPTS	VELOCITY M/S	INTERCEPT TIME, MS	MSE MS	CORREL COEFF
1	0.0	3.0	1	273.	-0.0	0.0	1.0000
2	3.0	27.0	9	465.	5.4	0.3	0.9978
3	27.0	36.0	4	1967.	49.8	0.5	0.7664

RSG-11 LINE 9-2 P WAVES

SEGMENT NO.	XMIN M	XMAX M	NPTS	VELOCITY M/S	INTERCEPT TIME, MS	MSE MS	CORREL COEFF
1	0.0	3.0	1	240.	-0.0	0.0	1.0000
2	3.0	27.0	9	448.	4.4	0.3	0.9966
3	27.0	36.0	4	1333.	43.8	0.2	0.9666

RSG-11 LINE 10-1 P WAVES

SEGMENT NO.	XMIN M	XMAX M	NPTS	VELOCITY M/S	INTERCEPT TIME, MS	MSE MS	CORREL COEFF
1	0.0	3.0	5	280.	-0.0	0.2	0.9960
2	3.0	27.0	14	460.	4.8	0.3	0.9968
3	27.0	36.0	4	1364.	44.9	0.3	0.9308

RSG-11 LINE 10-2 P WAVES

SEGMENT NO.	XMIN M	XMAX M	NPTS	VELOCITY M/S	INTERCEPT TIME, MS	MSE MS	CORREL COEFF
1	0.0	2.0	3	217.	-0.0	0.2	0.9958
2	2.0	27.0	17	452.	5.6	0.1	0.9991
3	27.0	36.0	4	2143.	53.3	0.2	0.9333

RSG-11 TEST SITE LINE 11-1 P WAVES

SEGMENT NO.	XMIN M	XMAX M	NPTS	VELOCITY M/S	INTERCEPT TIME, MS	MSE MS	CORREL COEFF
1	0.0	4.0	5	308.	0.0	0.1	0.9988
2	4.0	30.0	15	465.	2.9	0.2	0.9988
3	30.0	36.0	3	2400.	55.4	0.1	0.9865

RSG-11 TEST SITE LINE 11-2 P WAVES

SEGMENT NO.	XMIN M	XMAX M	NPTS	VELOCITY M/S	INTERCEPT TIME, MS	MSE MS	CORREL COEFF
1	0.0	4.0	5	310.	0.0	0.2	0.9984
2	4.0	27.0	14	442.	3.7	0.3	0.9967
3	27.0	36.0	4	1579.	48.3	0.3	0.9377

LINE 11-1 P WAVE PEAKS

3	30.0	36.0	5	1333	49.3	0.3	.8314

Table A3. P wave velocity structure.

Line	Spread Length (m)	Layer	Velocity (m s^{-1})	Thickness† A (m)	Thickness† B (m)	Dip** (deg)	Depth† A (m)	Depth† B (m)
1	36	1	233	0.3	0.3	-1.1	0.3	0.3
		2	424	8.7	11.7	-4.7	9.0	12.0
		3	1965					
2	63	1	233	1.0	0.5	0.4	1.0	0.5
		2	445	9.8	9.7	1.0	10.8	10.1
		3	1844					
3	36	1	203	1.6	0.8	0.7	1.6	0.8
		2	502	8.9	8.8	1.9	10.4	9.6
		3	1463					
4	36	1	203	0.6	0.7	-0.6	0.6	0.7
		2	487	7.7	10.0	-4.3	8.3	10.7
		3	1315					
5	36	1	217	1.0	0.7	0.3	1.0	0.7
		2	472	8.0	9.6	-1.8	9.0	10.4
		3	1394					
6	36	1	217	0.7	0.7	0.8	0.7	0.7
		2	465	9.2	10.3	-2.6	9.9	11.0
		3	1688					
7*	36	1	215	0.7	0.8	-0.2	0.7	0.8
		2	479	(12.3)	(2.5)	(16.0)	(12.9)	(3.3)
		3	(725)					
8*	36	1	215	0.5	0.8	-0.6	0.5	0.8
		2	501	10.3	12.9	-4.4	10.8	13.7
		3	1686					
9	36	1	248	0.8	0.7	0.7	0.8	0.7
		2	456	10.4	9.2	2.7	11.2	9.9
		3	1588					
10	36	1	248	0.7	0.8	0.3	0.7	0.8
		2	456	9.3	11.1	-3.9	10.0	11.9
		3	1663					
11	36	1	310	0.6	0.7	1.6	0.6	0.7
		2	449	10.8	10.4	-2.4	11.4	11.1
		3	1443					

Note * Lines 7 and 8 are affected by a low velocity anomaly. See text for discussion.
† A refers to forward profile (e.g., 1-1) at each site; B refers to the reversed profile (e.g., 1-2).
** A dip downward from A to B is negative.

Figures A1–A16. Graphs of travel time vs offset distance. Graphs for lines 1, 2, 4, 5, 6, 9, 10, and 11 are included here. Graphs for lines 3, 7, and 8 are contained in the body of the report.

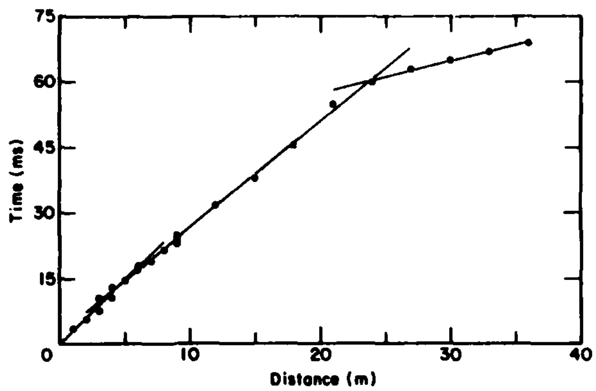

Figure A1. Line 1-1 P waves.

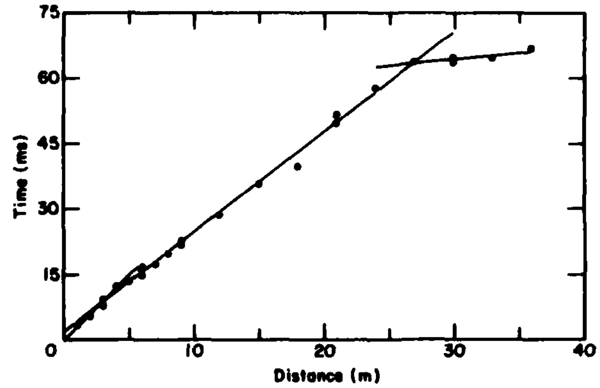

Figure A2. Line 1-2 P waves.

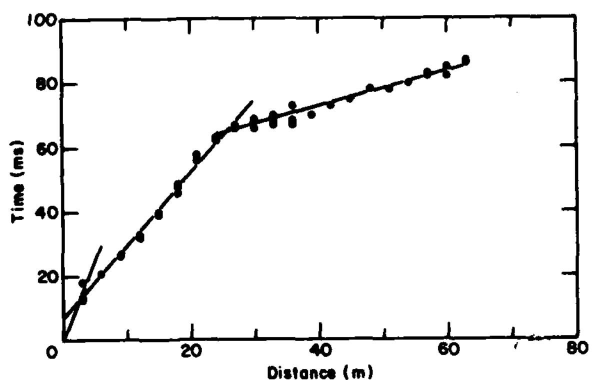

Figure A3. Line 2-1 P waves.

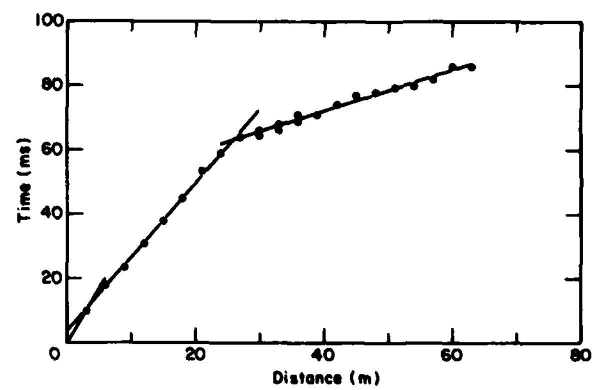

Figure A4. Line 2-2 P waves.

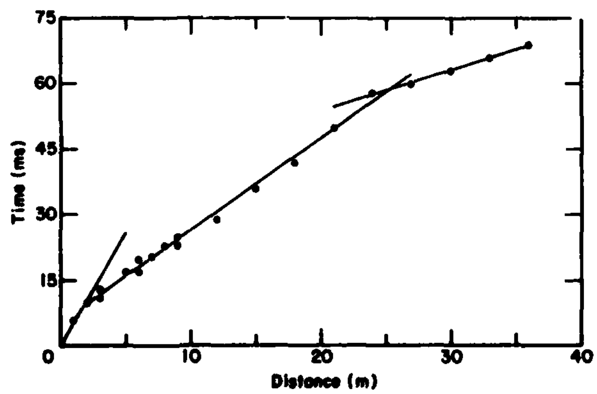

Figure A5. Line 4-1 P waves.

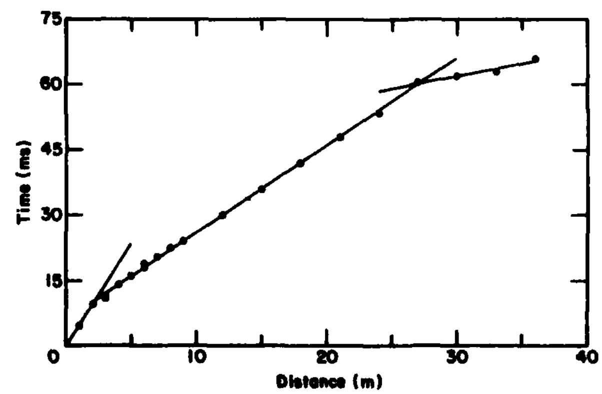

Figure A6. Line 4-2 P waves.

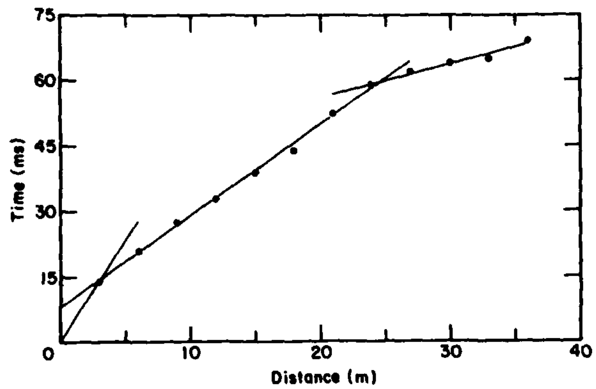

Figure A7. Line 5-1 P waves.

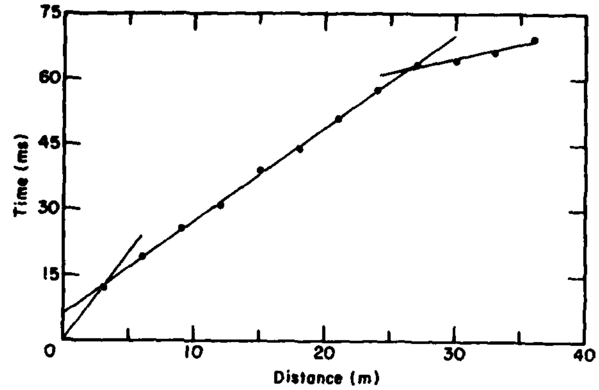

Figure A8. Line 5-2 P waves.

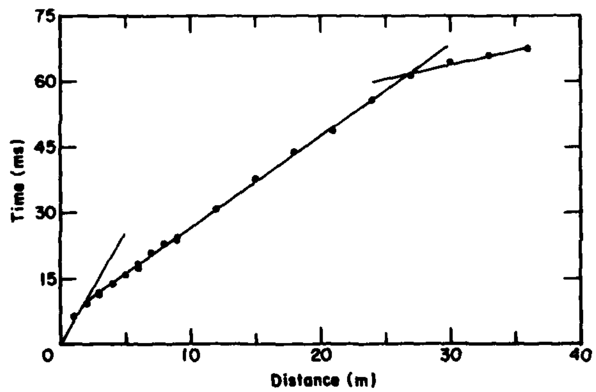

Figure A9. Line 6-1 P waves.

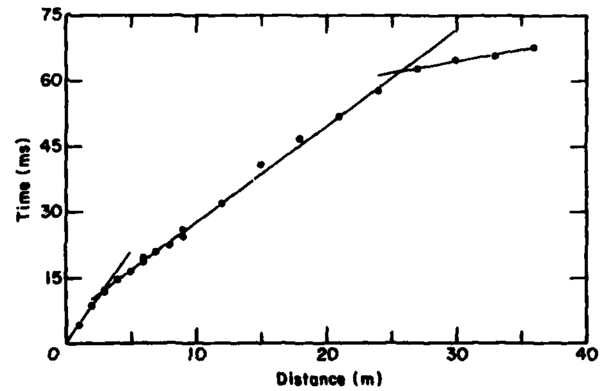

Figure A10. Line 6-2 P waves.

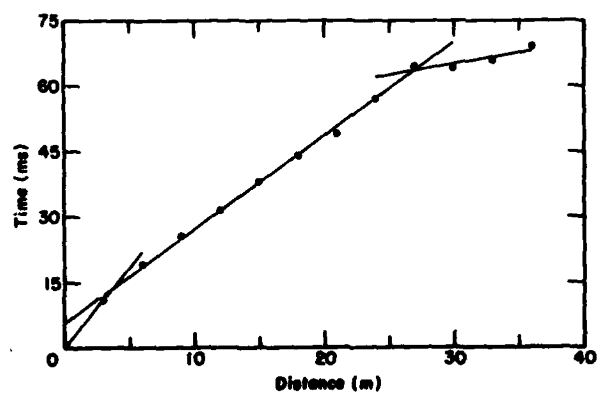

Figure A11. Line 9-1 P waves.

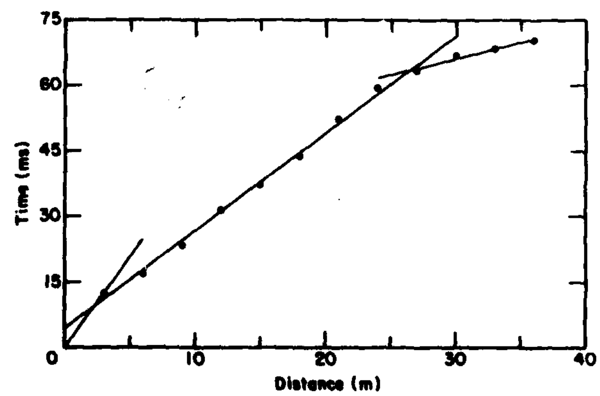

Figure A12. Line 9-2 P waves.

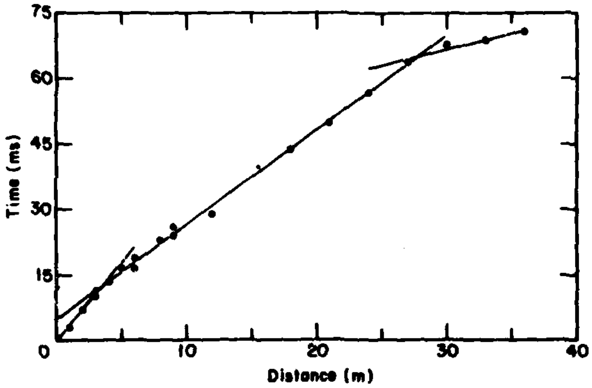

Figure A13. Line 10-1 P waves.

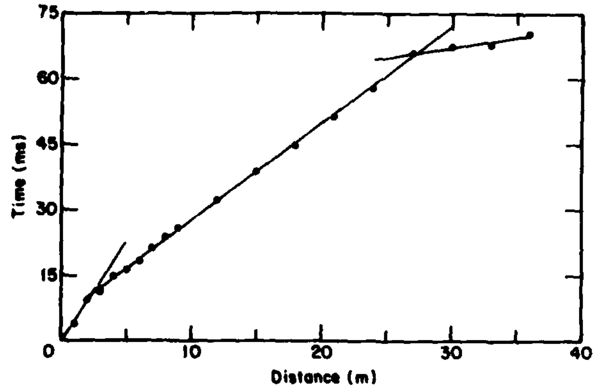

Figure A14. Line 10-2 P waves.

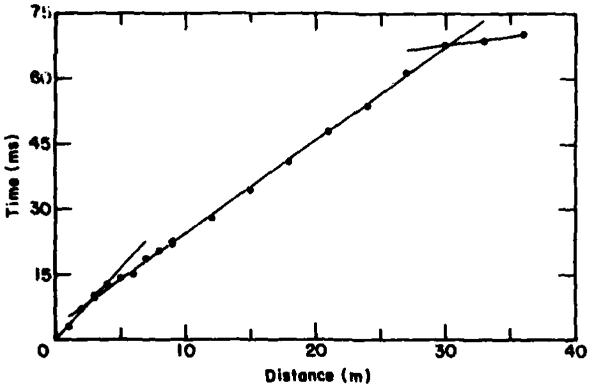

Figure A15. Line 11-1 P waves.

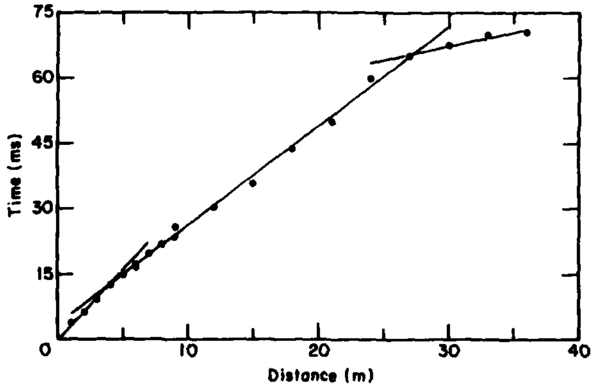

Figure A16. Line 11-2 P waves.

APPENDIX B: SH WAVE REFRACTION DATA

Table B1. SH wave refraction travel times and fitted line segment times. All distances are in meters; all times are in milliseconds. Symbols are the same as those in Appendix A. Lines 1-1, 1-2, 2-1, 2-2, 11-1, and 11-2 are listed.

RSG-11 LINE 1-1 SH WAVES

LINE SEGMENT NUMBER 1

X, M	T, MS	TLINE	DIFF
0.0	0.0	-0.0	0.0
3.0	18.0	18.2	-0.2
3.0	18.5	18.2	0.3
3.0	18.0	18.2	-0.2

LINE SEGMENT NUMBER 2

X, M	T, MS	TLINE	DIFF
3.0	18.0	20.2	-2.2
6.0	31.0	30.9	0.1
9.0	42.0	41.6	0.4
12.0	53.0	52.3	0.7
15.0	60.0	63.0	-3.0
18.0	74.5	73.7	0.8
21.0	90.0	84.4	5.6
30.0	116.0	116.6	-0.6
36.0	137.0	138.0	-1.0
3.0	18.5	20.2	-1.7
6.0	30.0	30.9	-0.9
9.0	42.0	41.6	0.4
12.0	53.0	52.3	0.7
15.0	62.5	63.0	-0.5
18.0	74.0	73.7	0.3
21.0	90.0	84.4	5.6
27.0	107.0	105.9	1.1
30.0	115.0	116.6	-1.6
33.0	125.0	127.3	-2.3
36.0	136.5	138.0	-1.5
3.0	18.0	20.2	-2.2
6.0	30.5	30.9	-0.4
9.0	42.0	41.6	0.4
12.0	52.0	52.3	-0.3
15.0	63.0	63.0	-0.0
18.0	74.0	73.7	0.3
21.0	89.0	84.4	4.6
24.0	97.5	95.2	2.3
30.0	114.5	116.6	-2.1
33.0	125.5	127.3	-1.8
36.0	137.0	138.0	-1.0

RSG-11 LINE 1-2 SH WAVES

LINE SEGMENT NUMBER 1

X, M	T, MS	TLINE	DIFF
0.0	0.0	-0.0	0.0
6.0	38.5	38.5	0.0

LINE SEGMENT NUMBER 2

X, M	T, MS	TLINE	DIFF
6.0	38.5	37.6	0.9
9.0	47.0	48.4	-1.4
12.0	62.0	59.3	2.7
15.0	73.0	70.1	2.9
18.0	86.0	80.9	5.1
21.0	94.0	91.7	2.3
24.0	102.0	102.6	-0.6
33.0	133.0	135.0	-2.0
36.0	143.0	145.9	-2.9
39.0	154.0	156.7	-2.7
42.0	169.0	167.5	1.5
45.0	177.5	178.3	-0.8
48.0	188.0	189.2	-1.2
51.0	200.0	200.0	0.0
33.0	133.0	135.0	-2.0
36.0	145.0	145.9	-0.9
39.0	154.0	156.7	-2.7
42.0	169.0	167.5	1.5
45.0	177.0	178.3	-1.3
48.0	190.0	189.2	0.8
51.0	199.0	200.0	-1.0
33.0	133.0	135.0	-2.0
36.0	146.0	145.9	0.1
39.0	155.0	156.7	-1.7
42.0	169.0	167.5	1.5
45.0	177.0	178.3	-1.3
48.0	188.0	189.2	-1.2
51.0	199.0	200.0	-1.0
54.0	212.0	210.8	1.2
57.0	219.5	221.6	-2.1
63.0	241.0	243.3	-2.3
66.0	262.0	254.1	7.9
54.0	208.0	210.8	-2.8
57.0	221.0	221.6	-0.6
60.0	235.0	232.5	2.5
63.0	246.0	243.3	2.7
66.0	257.0	254.1	2.9
54.0	208.0	210.8	-2.8
57.0	220.0	221.6	-1.6
60.0	232.0	232.5	-0.5
63.0	247.0	243.3	3.7
66.0	256.0	254.1	1.9
69.0	262.5	264.9	-2.4

LINE SEGMENT NUMBER 3

X, M	T, MS	TLINE	DIFF
69.0	262.5	260.1	2.4
72.0	265.0	265.2	-0.2
78.0	272.0	275.5	-3.5
81.0	279.0	280.6	-1.6
84.0	286.0	285.7	0.3
87.0	293.5	290.9	2.6

RSG-11 LINE 2-1 SH WAVES

LINE SEGMENT NUMBER 1

X, M	T, MS	TLINE	DIFF
0.0	0.0	-0.0	0.0
3.0	26.0	25.5	0.5
3.0	25.0	25.5	-0.5

LINE SEGMENT NUMBER 2

X, M	T, MS	TLINE	DIFF
3.0	26.0	28.5	-2.5
6.0	36.0	38.4	-2.4
9.0	43.0	48.3	-5.3
12.0	52.5	58.1	-5.6
15.0	68.0	68.0	0.0
18.0	79.5	77.8	1.7
21.0	90.0	87.7	2.3
24.0	101.0	97.6	3.4
27.0	110.5	107.4	3.1
30.0	117.0	117.3	-0.3
33.0	128.0	127.2	0.8
36.0	141.0	137.0	4.0
3.0	25.0	28.5	-3.5
6.0	36.0	38.4	-2.4
9.0	44.0	43.3	-4.3
12.0	50.0	58.1	-8.1
18.0	79.0	77.8	1.2
24.0	104.0	97.6	6.4
27.0	111.0	107.4	3.6
30.0	120.0	117.3	2.7

33.0	129.0	127.2	1.8
36.0	142.0	137.0	5.0
33.0	133.0	127.2	5.8
36.0	145.0	137.0	8.0
39.0	149.0	146.9	2.1
42.0	155.0	156.7	-1.7
33.0	130.0	127.2	2.8
36.0	143.0	137.0	6.0
45.0	165.0	166.6	-1.6
51.0	186.0	186.3	-0.3
54.0	195.0	196.2	-1.2
57.0	201.0	206.1	-5.1
60.0	215.0	215.9	-0.9
63.0	220.0	225.8	-5.8
66.0	226.0	235.6	-9.6

RSG-11 LINE 2-2 SH WAVES

LINE SEGMENT NUMBER 1

X, M	T, MS	TLINE	DIFF
0.0	0.0	0.0	-0.0
3.0	20.0	20.0	0.0
3.0	20.0	20.0	0.0

LINE SEGMENT NUMBER 2

X, M	T, MS	TLINE	DIFF
3.0	20.0	22.8	-2.8
6.0	30.0	33.5	-3.5
9.0	42.0	44.3	-2.3
12.0	56.0	55.0	1.0
15.0	70.0	65.7	4.3
18.0	80.0	76.5	3.5
21.0	89.5	87.2	2.3
24.0	100.5	97.9	2.6
27.0	109.5	108.7	0.8
30.0	122.0	119.4	2.6
33.0	131.0	130.1	0.9
36.0	143.0	140.8	2.2
3.0	20.0	22.8	-2.8
6.0	34.0	33.5	0.5
9.0	45.0	44.3	0.7
12.0	56.0	55.0	1.0
15.0	68.0	65.7	2.3
18.0	82.5	76.5	6.0
21.0	88.0	87.2	0.8
24.0	97.0	97.9	-0.9
27.0	104.0	108.7	-4.7
30.0	117.5	119.4	-1.9
33.0	130.0	130.1	-0.1
36.0	143.0	140.8	2.2
33.0	123.0	130.1	-7.1
45.0	178.0	173.0	5.0
33.0	125.0	130.1	-5.1
36.0	135.0	140.8	-5.8
39.0	150.0	151.6	-1.6

RSG-11 TEST SITE LINE 11-1 SH WAVES

LINE SEGMENT NUMBER 1

X, M	T, MS	TLINE	DIFF
0.0	0.0	-0.0	0.0
1.0	6.0	6.4	-0.4
2.0	13.0	12.8	0.2

LINE SEGMENT NUMBER 2

X, M	T, MS	TLINE	DIFF
3.0	17.0	16.4	0.6
3.0	19.0	16.4	2.6
4.0	20.0	20.2	-0.2
5.0	24.5	23.9	0.6
6.0	27.0	27.6	-0.6
6.0	29.0	27.6	1.4
7.0	30.0	31.3	-1.3
8.0	34.0	35.0	-1.0
9.0	37.5	38.8	-1.3
9.0	39.0	38.8	0.2
12.0	50.0	49.9	0.1
15.0	59.0	61.1	-2.1
18.0	70.0	72.2	-2.2
21.0	81.0	83.4	-2.4
24.0	99.0	94.6	4.4
27.0	108.0	105.7	2.3
30.0	117.0	116.9	0.1
33.0	127.0	128.0	-1.0
36.0	139.0	139.2	-0.2

RSG-11 LINE 11-2 SH WAVES

LINE SEGMENT NUMBER 1

X, M	T, MS	TLINE	DIFF
0.0	0.0	-0.0	0.0
1.0	5.3	5.7	-0.5
2.0	12.0	11.4	0.6
3.0	17.0	17.1	-0.1
3.0	17.0	17.1	-0.1

LINE SEGMENT NUMBER 2

X, M	T, MS	TLINE	DIFF
3.0	17.0	16.9	0.1
3.0	17.0	16.9	0.1
4.0	19.0	20.9	-1.9
5.0	25.0	24.9	0.1
6.0	28.5	28.9	-0.4
6.0	30.0	28.9	1.1
6.0	29.0	28.9	0.1
7.0	33.0	32.8	0.2
8.0	36.5	36.8	-0.3
9.0	40.0	40.8	-0.8
9.0	41.0	40.8	0.2
9.0	41.0	40.8	0.2
12.0	52.0	52.7	-0.7
12.0	51.0	52.7	-1.7
15.0	65.0	64.7	0.3
15.0	64.0	64.7	-0.7
18.0	77.0	76.6	0.4
18.0	78.0	76.6	1.4
21.0	89.0	88.6	0.4
21.0	89.0	88.6	0.4
24.0	102.0	100.5	1.5
24.0	102.0	100.5	1.5
27.0	115.0	112.4	2.6
30.0	125.0	124.4	0.6
30.0	125.0	124.4	0.6
33.0	137.0	136.3	0.7
33.0	135.0	136.3	-1.3
36.0	146.0	148.3	-2.3
36.0	146.0	148.3	-2.3

Table B2. Fitted line segments for all SH refraction lines.

RSG-11 LINE 1-1 SH WAVES

SEGMENT NO.	XMIN M	XMAX M	NPTS	VELOCITY M/S	INTERCEPT TIME, MS	MSE MS	CORREL COEFF
1	0.0	3.0	4	165.	-0.0	0.1	0.9998
2	3.0	36.0	31	280.	9.5	0.4	0.9970

RSG-11 LINE 1-2 SH WAVES

SEGMENT NO.	XMIN M	XMAX M	NPTS	VELOCITY M/S	INTERCEPT TIME, MS	MSE MS	CORREL COEFF
1	0.0	6.0	2	156.	-0.0	0.0	1.0000
2	6.0	69.0	43	277.	16.0	0.4	0.9984
3	69.0	87.0	6	585.	142.1	0.9	0.9624

RSG-11 LINE 2-1 SH WAVES

SEGMENT NO.	XMIN M	XMAX M	NPTS	VELOCITY M/S	INTERCEPT TIME, MS	MSE MS	CORREL COEFF
1	0.0	3.0	3	118.	-0.0	0.2	0.9996
2	3.0	66.0	35	304.	18.7	0.7	0.9946

RSG-11 LINE 2-2 SH WAVES

SEGMENT NO.	XMIN M	XMAX M	NPTS	VELOCITY M/S	INTERCEPT TIME, MS	MSE MS	CORREL COEFF
1	0.0	3.0	3	150.	0.0	0.0	1.0000
2	3.0	45.0	29	280.	12.1	0.6	0.9941

RSG-11 TEST SITE LINE 11-1 SH WAVES

SEGMENT NO.	XMIN M	XMAX M	NPTS	VELOCITY M/S	INTERCEPT TIME, MS	MSE MS	CORREL COEFF
1	0.0	2.5	3	156.	-0.0	0.1	0.9990
2	2.5	36.0	19	269.	5.3	0.4	0.9981

RSG-11 LINE 11-2 SH WAVES

SEGMENT NO.	XMIN M	XMAX M	NPTS	VELOCITY M/S	INTERCEPT TIME, MS	MSE MS	CORREL COEFF
1	0.0	3.0	5	175.	-0.0	0.2	0.9992
2	3.0	36.0	29	251.	5.0	0.2	0.9993

Table B3. SH wave velocity structure for all refraction lines.

	Spread length (m)		Velocity $m\ s^{-1}$	Thickness (m) A	Thickness (m) B	Dip (deg)	Depth A	Depth B
1	87	1	165	1.0	1.6		1.0	1.6
		2	279	(20.7)	(19.5)	0.2	(21.7)	(21.1)
		3	(585)			(−0.2)		
2	66	1	165	1.9	1.2		1.9	1.2
		2	291			1.6		
11	36	1	166	0.6	0.5		0.6	0.5
		2	260			1.6		

Figures B1–B4. Graphs of SH wave travel time vs. offset distance. Graphs for lines 1-1, 1-2, 2-1, and 2-2 are included here. Graphs for line 11 are given in the main body of this report.

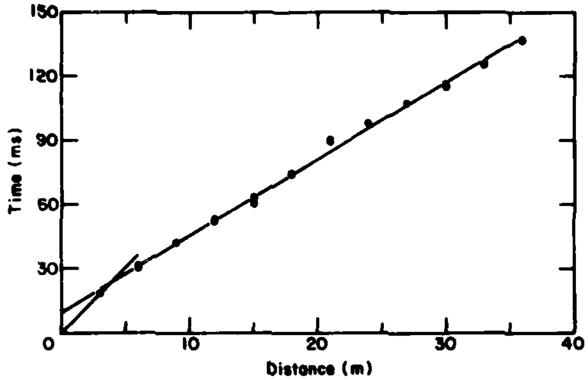

Figure B1. Line 1-1 SH waves.

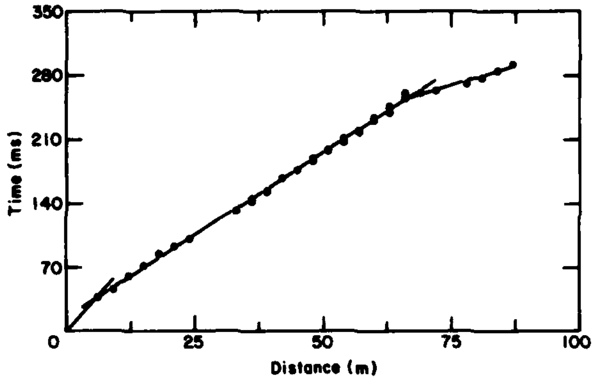

Figure B2. Line 1-2 SH waves.

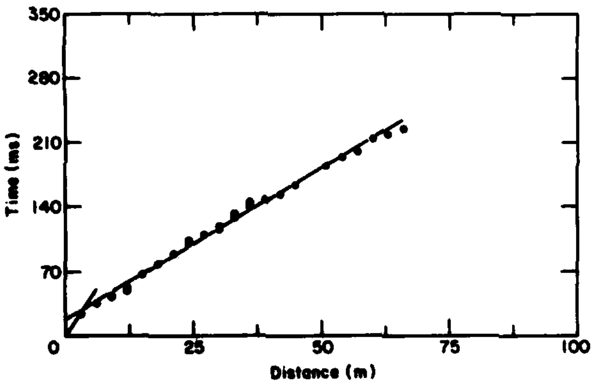

Figure B3. Line 2-1 SH waves.

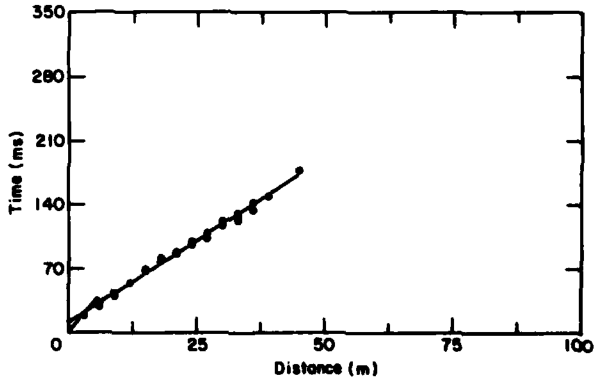

Figure B4. Line 2-2 SH waves.

APPENDIX C: SURFACE WAVE DISPERSION CALCULATIONS

Table C1. Theoretical group and phase velocity dispersion for model A (based on average properties).

a. Model A.

Thickness (m)	P velocity ($m\ s^{-1}$)	SH velocity ($m\ s^{-1}$)	Density ($g\ cm^{-3}$)
1.1	238	165	1.9
9.5	467	276	2.0
10.0	1590	276	2.1
∞	1590	585	2.2

b. Love wave dispersion, fundamental mode.

Period (s)	Frequency (Hz)	Phase Velocity ($m\ s^{-1}$)	Group Velocity ($m\ s^{-1}$)
.020	50	210	155
.022	45	218	159
.024	42	225	165
.026	38	231	172
.028	36	237	180
.030	33	242	188
.032	31	246	196
.034	29	249	204
.036	28	252	210
.038	26	255	215
.040	25	257	223
.042	24	259	228

Table C2. Theoretical group and phase velocity dispersion for model B (based on line 2-2 refraction velocities).

a. Model B.

Thickness (m)	P velocity ($m\ s^{-1}$)	SH velocity ($m\ s^{-1}$)	Density ($g\ cm^{-3}$)
1.1	233	150	1.9
9.5	436	280	2.0
10.0	1590	280	2.1
∞	1590	585	2.2

b. Love wave dispersion, fundamental mode.

Period (s)	Frequency (Hz)	Phase Velocity ($m\ s^{-1}$)	Group Velocity ($m\ s^{-1}$)
.020	50	183	104
.022	45	190	113
.024	42	198	121
.026	38	205	129
.028	36	213	136
.030	33	221	144
.032	31	227	153
.034	29	233	162
.036	28	239	172
.038	26	244	181
.040	25	248	189
.042	24	251	197

A facsimile catalog card in Library of Congress MARC format is reproduced below.

Albert, Donald G.
Seismic site characterization techniques applied to the NATO RSG-11 test site in Münster Nord, Federal Republic of Germany / by Donald G. Albert. Hanover, N.H.: U.S. Cold Regions Research and Engineering Laboratory; Springfield, Va.: available from National Technical Information Service, 1982.
iv, 37 p., illus.; 28 cm. (CRREL Report 82-17.)
Prepared for Office of the Chief of Engineers by Corps of Engineers, U.S. Army Cold Regions Research and Engineering Laboratory under DA Project 4A762730 AT42.
Bibliography: p. 14.

Albert, Donald G.
Seismic site characterization techniques...
1982. (Card 2)

1. Geologic models. 2. NATO. 3. Seismic refraction. 4. Seismic signatures. 5. Seismic surface waves. 6. Seismology. 7. West Germany. I. United States. Army. Corps of Engineers. II. Army Cold Regions Research and Engineering Laboratory, Hanover, N.H. III. Series: CRREL Report 82-17.

☆U.S. GOVERNMENT PRINTING OFFICE: 1982 – A-2294/165

DATE
ILMED

8